Three-dimensional finite element analysis of initial displacement and stress on the craniofacial structures of unilateral cleft lip and palate model during protraction therapy with variable forces and directions

Shahistha Parveen , Akhter Husain , Srinivas Gosla Reddy , Rohan Mascarenhas & Satish Shenoy

Published online: 02 Sep 2020.

Submit your article to this journal ↗

View related articles ↗

View Crossmark data ↗

Check for updates

Three-dimensional finite element analysis of initial displacement and stress on the craniofacial structures of unilateral cleft lip and palate model during protraction therapy with variable forces and directions

Shahistha Parveen[a] [iD], Akhter Husain[a], Srinivas Gosla Reddy[b], Rohan Mascarenhas[a] and Satish Shenoy[c]

[a]Department of Orthodontics and Dentofacial Orthopedics, Yenepoya Dental College, Yenepoya (Deemed to be University), Mangalore, Karnataka, India; [b]GSR Institute of Craniomaxillofacial and Facial Plastic Surgery, Hyderabad, Telangana, India; [c]Manipal Institute of Technology, Department of Aeronautical & Automobile Engineering, MAHE (Deemed to be University), Manipal, Karnataka, India

ABSTRACT

Maxillary protraction and expansion is recommended to treat midfacial deficiency in patients with cleft lip and palate (CLP), where amount and direction of forces can change displacement and stress. This study assessed the initial displacement and stresses using Facemask and Maxgym forces with and without RME at $+20°$, $0°$, and $-20°$ angulation using a finite element (FE) model of unilateral cleft lip and palate (UCCLP). The Initial displacement and stress were more for protraction with expansion as compared to only protraction. Asymmetric displacement was observed with more on cleft than on noncleft side and more on dental than skeletal structures. Palatal plane rotated less upward, increased arch width and decreased arch length was observed with protraction with expansion.

Introduction

Cleft lip and palate (CLP) is one of the most common birth deformities which results from the failure of fusion of the maxillary and palatine processes (Cobourne 2004). Cleft can involve both lip and palate, either lip or palate. Based on the type and site of involvement, it can be classified as complete or incomplete, unilateral or bilateral.

Although primary CLP repair during infancy and early childhood improves facial appearance and functional development, it can cause midfacial growth deficiency (Liao and Mars 2005). The midfacial discrepancy can be treated by protraction and expansion. Maxillary protraction appliances are used to correct the sagittal discrepancies, and expansion appliances are used to correct the transverse discrepancy. Studies have shown that protraction with expansion has a synergistic effect (Tindlund 1994; Dogan 2012).

Corrections achieved using facemask in patients with UCCLP during early age may reduce the severity of skeletal defect (Molsted and Dahl 1987; Tindlund 1994; Dogan 2012). Though skeletal correction is desirable, protraction also brings about changes in dental structures. Facemask (FM) is a conventional maxillary protraction appliance used in individuals with CLP (Molsted and Dahl 1987; Buschang et al. 1994; Kawakami et al. 2002; Dogan 2012). Maxgym (MG) is a new protraction device designed to treat midfacial deficiency using variable weights on a pulley (Figure 1) (Patent application number: 2303/CHE/2011).

The rapid maxillary expansion (RME) screw is incorporated into the splint, which is cemented to the first molars and premolars. FM is placed on the patient, and the forehead pad and chin cap are adjusted according to the patient's face. The elastics are worn from the crossbar to the hooks on the splint between the premolars at different angles depending on the needs. The MG is mounted on the wall, preferably in the residence of the patient at a suitable position depending on the height of the patient. The handles help the patient to grip the MG comfortably while doing this exercise. The patient is trained to connect the free ends of the wire from the pulley of the device to the hooks placed on the splint cemented intraorally. The patient is asked to gently pull away from MG at required directions which may be upward, downward, and parallel. This principle of pulling force on the maxillary structure is simple and
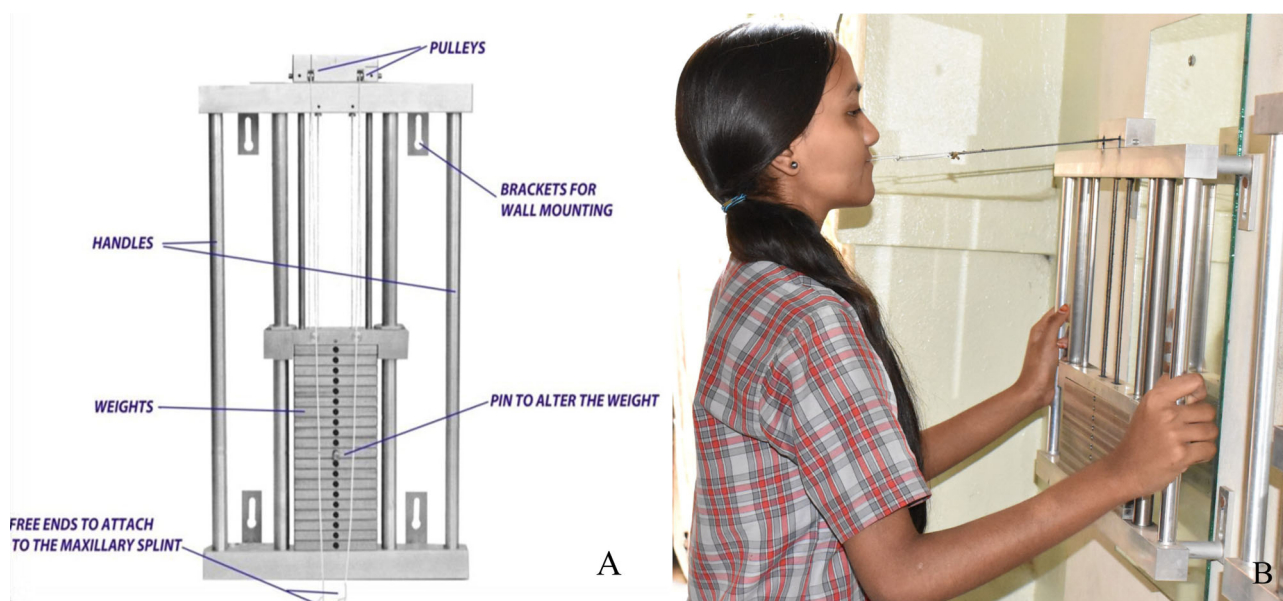

Figure 1. Maxgym A. Labeled model B. Patient using mounted Maxgym.

mechanically sound enough to be used as a therapeutic procedure in the treatment of maxillary deficiency. Once the patient is identified, the amount of force and duration is standardized under the supervision of a trained orthodontist.

Several finite element method (FEM) studies have been conducted to investigate the effect of maxillary protraction forces on craniofacial structures in individuals with CLP (Yang et al. 2012; Chen et al. 2013, 2015; Zhang et al. 2015). Studies also indicated that different directions and points of application of protraction forces influence distribution of stress and displacement pattern (Itoh et al. 1985; Hata et al. 1987; Tanne and Sakuda 1991; Grandori et al. 1992; Keles et al. 2002; Yepes et al. 2014). Parallel traction produced counterclockwise rotation of maxilla, and downward pull reduces the rotation (Itoh et al. 1985; Tanne and Sakuda 1991; Grandori et al. 1992). Force vector parallel to the occlusal plane produced compressive stresses in the bones around the maxillofacial sutures, in addition to the tensile stresses in the maxillary bone, which results in counterclockwise (CCW) rotation of the maxilla and can be minimized by more downward and anteriorly directed force (Grandori et al. 1992).

Some researchers also reported protraction forces above the occlusal plane maxillary advancement with minimum rotation. Hata et al. (1987) recommended to use protraction forces 5 mm above the palatal plane to avoid rotation of the maxilla. However, in deep bite cases, protraction forces can be kept at the level of maxillary arch to open the bite. Keles et al. (2002)

reported that maxilla advanced forward with a counterclockwise rotation for force vector at $-30°$ to the occlusal plane whereas the force applied 20 mm above the maxillary occlusal plane brings about translatory movement of the maxilla.

The FM uses anchorage from the forehead and chin, whereas the MG is anchored to the wall. Although the site of anchorage was different for the MG and FM, the point of application of force on the splint was the same. The advantages of MG over FM are patient's compliance and lesser duration of wear. The aim of this study was to simulate FM and MG forces with and without expansion in a UCCLP model to analyze stress and displacement of craniofacial structures at $+20°$, $0°$, and $-20°$ to the occlusal plane using finite element analysis (FEA).

Materials and methods

After ethical clearance was obtained from the ethics committee of our university (YUEC 2017/310), the model used for the construction of FE model was generated from computed tomography (CT) images of the skull, obtained with bright speed 16/Helical multislice, GE Healthcare. The specifications of machine are as follows: 0.625 slice thickness, $0.35 \times 0.35 \times 0.35 \, mm^3$ isotropic voxel size, 120 kV, 300 mA, 512×512 matrix, FOV (head type), scan time: 20 s, exposure time: 21.3 s. The CT images were exported as uncompressed Digital Imaging and Communications in Medicine (DICOM) files.
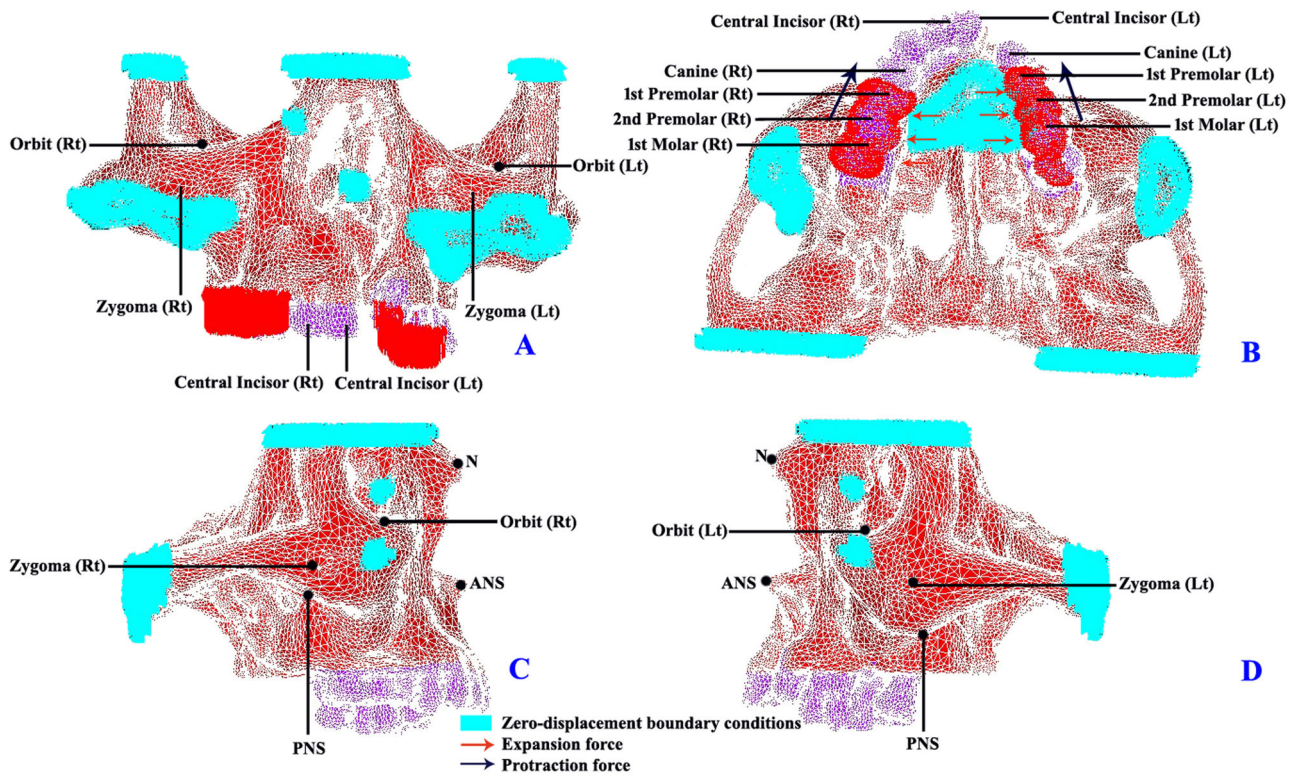
Figure 2. Different views of FE Model with defined boundary condition and marker nodes representing the dental and skeletal structure; different views: A. Frontal, B. Occlusal, C. Right buccal, and D. Left buccal.

Table 1. Young's modulus and Poisson's ratio.

	Young's modulus (kg/mm^2)	Poisson's ratio
Cancellous bone	1.3×10^3	0.3
Compact bone	7.9×10^3	0.3
Tooth	2.0×10^4	0.3

DICOM files were obtained from the CT scan of a patient with unilateral cleft lip and palate (UCCLP) on the left side and were imported into Mimics® software version 18 (Materialise NV, Leuven, Belgium) for construction of FE model. FE model was generated from a geometric model consisting of 49,807 nodes and 185,620 tetrahedral shaped elements (Figure 2). Mesh dependency check was carried out for validation of the model, which showed that optimum mesh sizes had been used. Displacement identified by using these mesh sizes showed variations of less than 1%. Numerical validation of model was then carried out with data from previous studies (Yang et al. 2012; Chen et al. 2013; Zhang et al. 2015). The mechanical properties of the cortical bone, cancellous bone, and teeth in the model were defined based on the data from previous studies (Table 1) (Yu et al. 2007; Gautam et al. 2009; Yang et al. 2012; Chen et al. 2013, 2015; Zhang et al. 2015; Eom et al. 2018). Materials in the analysis were assumed to be linearly elastic and isotropic.

Zero-displacement boundary conditions were designated on the suitable outer extremities of the model so as to facilitate analysis of changes which happens within the craniofacial structures. The boundary conditions were designated on the suitable outer extremities of the model so as to facilitate analysis of changes which happens within the craniofacial structures. Since this is a model of UCCLP, the cleft divides the maxilla into unequal parts, and the resultant stress and displacement can be studied more accurately.

Hence, FEA allows us to study the effects of protraction forces with and without expansion and in different directions where the properties of tooth, bone, etc. can also be changed. Therefore, one model was sufficient to simulate different clinical situations.

The MG philosophy is to use higher forces for a shorter time. It was designed to deliver higher forces as compared to FM, which was to be worn for a longer time. The range of forces used in this study was from published literature. The higher forces simulated MG and lower forces simulated FM (Tanne et al. 1989; Grandori et al. 1992; Keles et al. 2002; Vaughn et al. 2005; Tortop et al. 2007; Proffit et al. 2013). In this study, FM was represented with light protraction force of 600 g (300 g per side), and MG was represented with heavy protraction force of 1200 g (600 g per side). Holberg et al. (2007) reported that the use of an RME appliance with
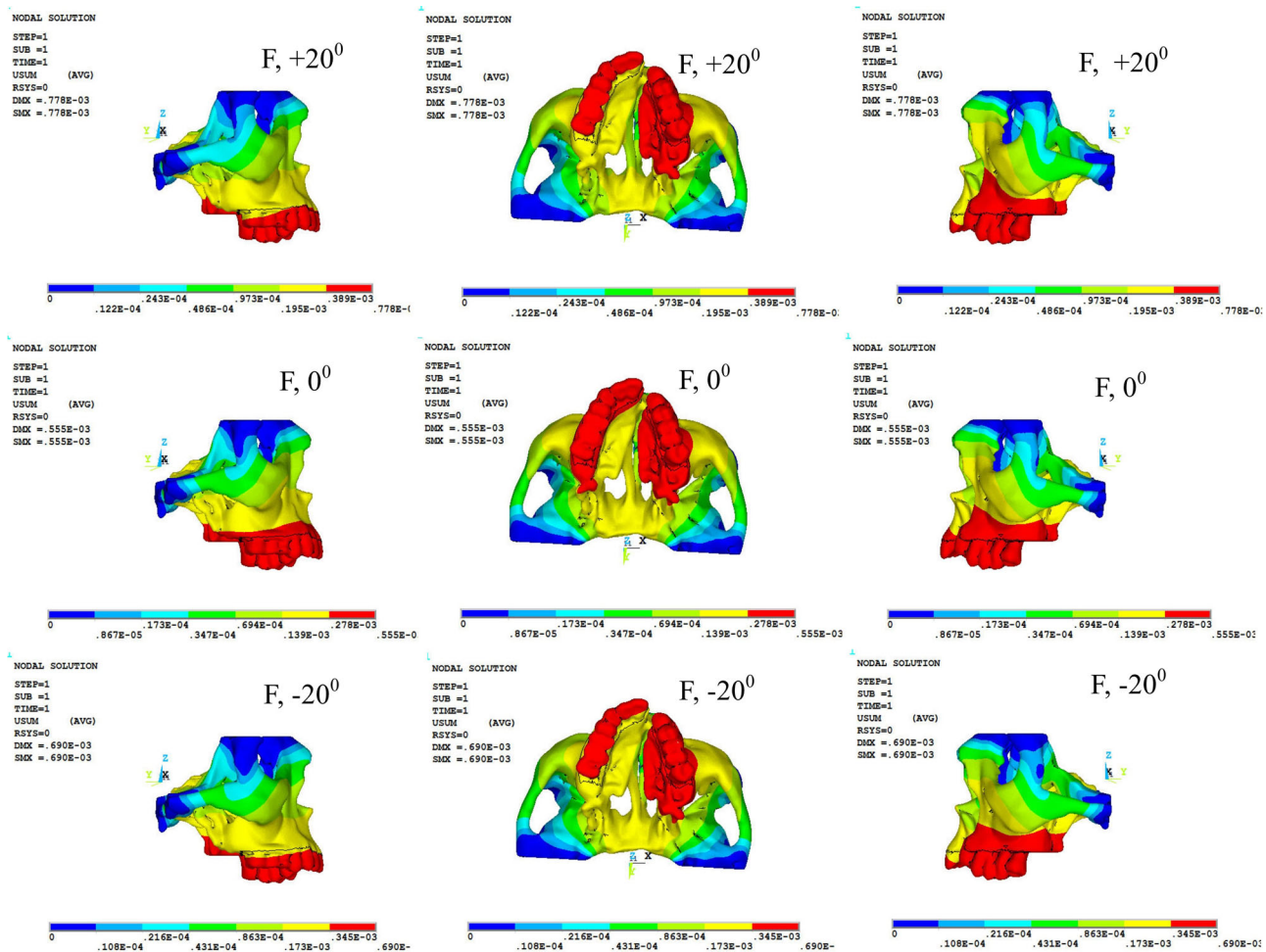
Figure 3. Initial displacement of craniofacial structures with only facemask forces.

heavy forces is not required for cleft patients, and orthodontic force of 5 N or less is sufficient to bring about skeletal expansion. Simulated forces for RME used in the current study were E = 500 g per side, which were selected based on previous study (Mathew et al. 2016).

FM and MG protraction forces were applied from the middle of the clinical crown on the buccal side of the first premolars at +20°, 0°, and −20° to the occlusal plane. The RME forces were divided as follows: 50% on the premolar region and 50% on the molar region (Figure 2). The RME force was applied to the middle of the crown length on the palatal side of the first premolars and the first molars.

The distribution of stress and displacement of the craniofacial structures was assessed using 23 marker nodes out of which 14 were dental structures and nine were skeletal structures. The dental marker nodes to be analyzed were located on cleft (C) and noncleft (NC) sides of molar cusps (n = 2), molar root apices (n = 2), premolar cusps (n = 2), premolar root apices (n = 2), canine cusp tips (n = 2), C = central incisor (n = 2), and central incisor root apices (n = 2). The skeletal nodes

were located on ANS (n = 1), PNS (n = 1), point A (n = 1), subnasale (n = 1), nasal bone (n = 1), orbits (n = 2), and zygoma (n = 2).

The pattern of initial displacement and distribution of von Mises stresses were analyzed in the UCCLP model by simulating twelve clinical situations consisting of the following: 1. protraction only (1. F, +20°; 2. F, 0°; 3. F, −20°; 4. M, +20°; 5. M, 0°; 6. M, −20°) and 2. combinations of protraction and expansion (7. F, E, +20°; 8. F, E, 0°; 9. F, E, −20°; 10. M, E, +20°; 11. M, E, 0°; 12. M, E, −20°).

Changes in intercanine width (ICW), intermolar width (IMW), and palatal plane length (PPL) were calculated using distance formula $[d = \sqrt{(x_2-x_1)^2 + (y_2-y_1)^2}]$ to assess net change in the linear distance by calculating displacement along three axes at two points A (x_1, y_1) and B (x_2, y_2).

Results

The analysis was carried out using ANSYS software (ANSYS 19; Inc., Canonsburg, PA). The results were
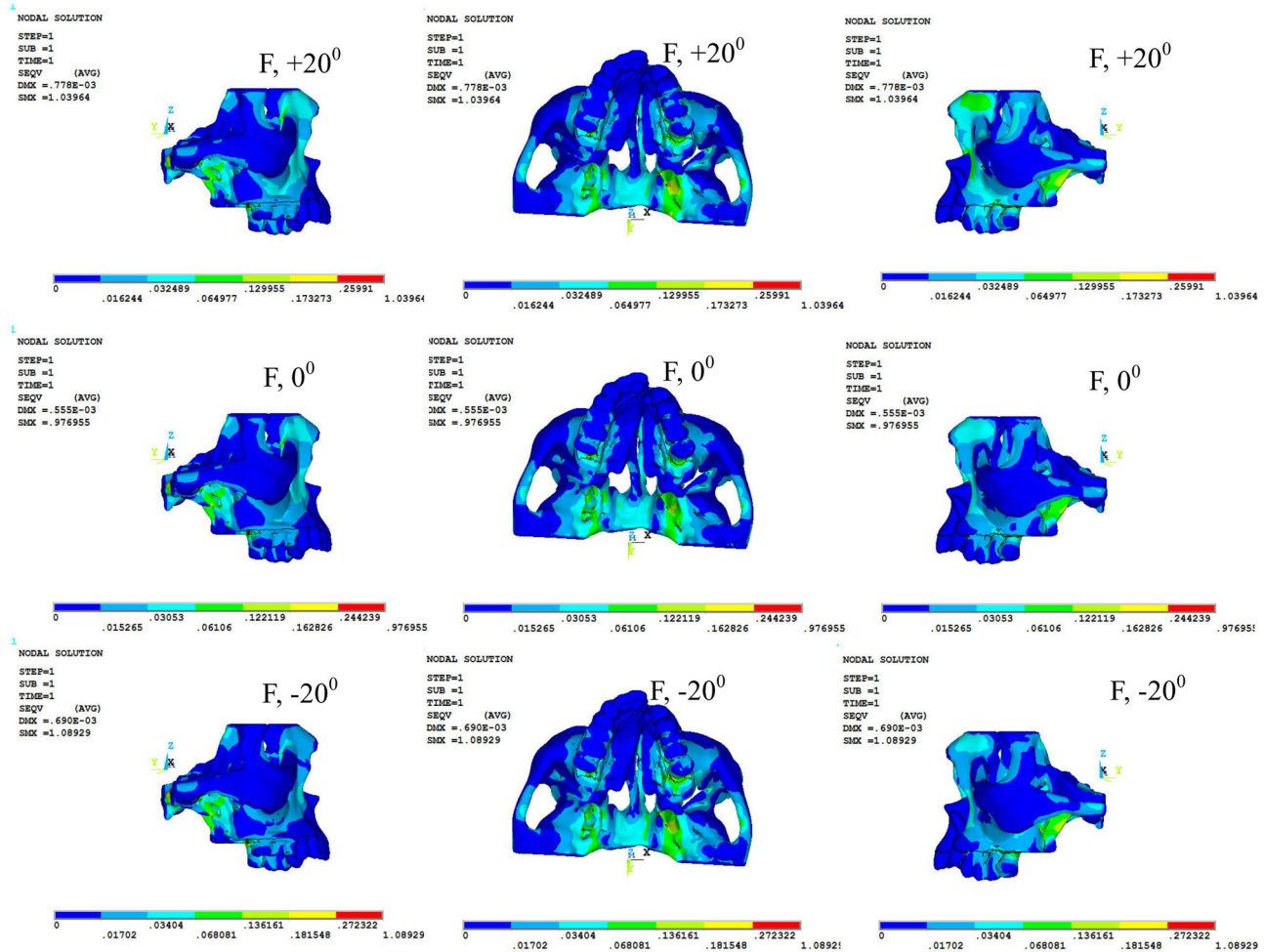
Figure 4. Distribution of stress on craniofacial structures with only facemask forces.

obtained in a band with different colors, indicating various levels of stress and initial displacement. The red color indicated structures with the highest and blue color indicated the structure with the lowest stress or initial displacement (Figures 3–10). The directional analysis was used for the presentation of results. Values were recorded in all three co-ordinate axes which were defined as X-axis (transverse), Y-axis (sagittal), and Z-axis (vertical) (Tables 2–5). Initial displacement along different axes can be interpreted as follows. X-axis: Negative and positive values have different interpretations on the right and left sides. Right side (noncleft side): Positive value indicated medial movement (M) and a negative value indicated lateral movement (L). Left side (cleft side): Negative value indicated medial movement (M) and a positive value indicated lateral movement (L). The movements of midline structures along X-axis were denoted by right (Rt) and left (Lt) side movement for negative and positive values. Y-axis: Negative value indicated forward movement (F) and the positive value indicated backward movement (B). Z-axis: Negative value

indicated downward movement (D) and a positive value indicated upward movement (U).

Analysis of initial displacement in transverse direction (X-axis)

The displacement of craniofacial structures in the transverse direction was more with protraction and expansion as compared to only protraction (Tables 2–5) (Figures 3, 5, 7, and 9). Dental structures displaced more as compared to skeletal structures, and displacement of structures on the cleft side was more as compared to noncleft side. All skeletal structures displaced laterally (expansion) except for right zygoma which moved medially during protraction with and without expansion. For protraction-only forces, +20° produced greater initial displacement as compared to 0°, or −20°. The displacement had a minimal variation for protraction with expansion irrespective of the angulation of force application. Intercanine width (ICW), which represents anterior expansion, and intermolar width (IMW), which represents posterior expansion,
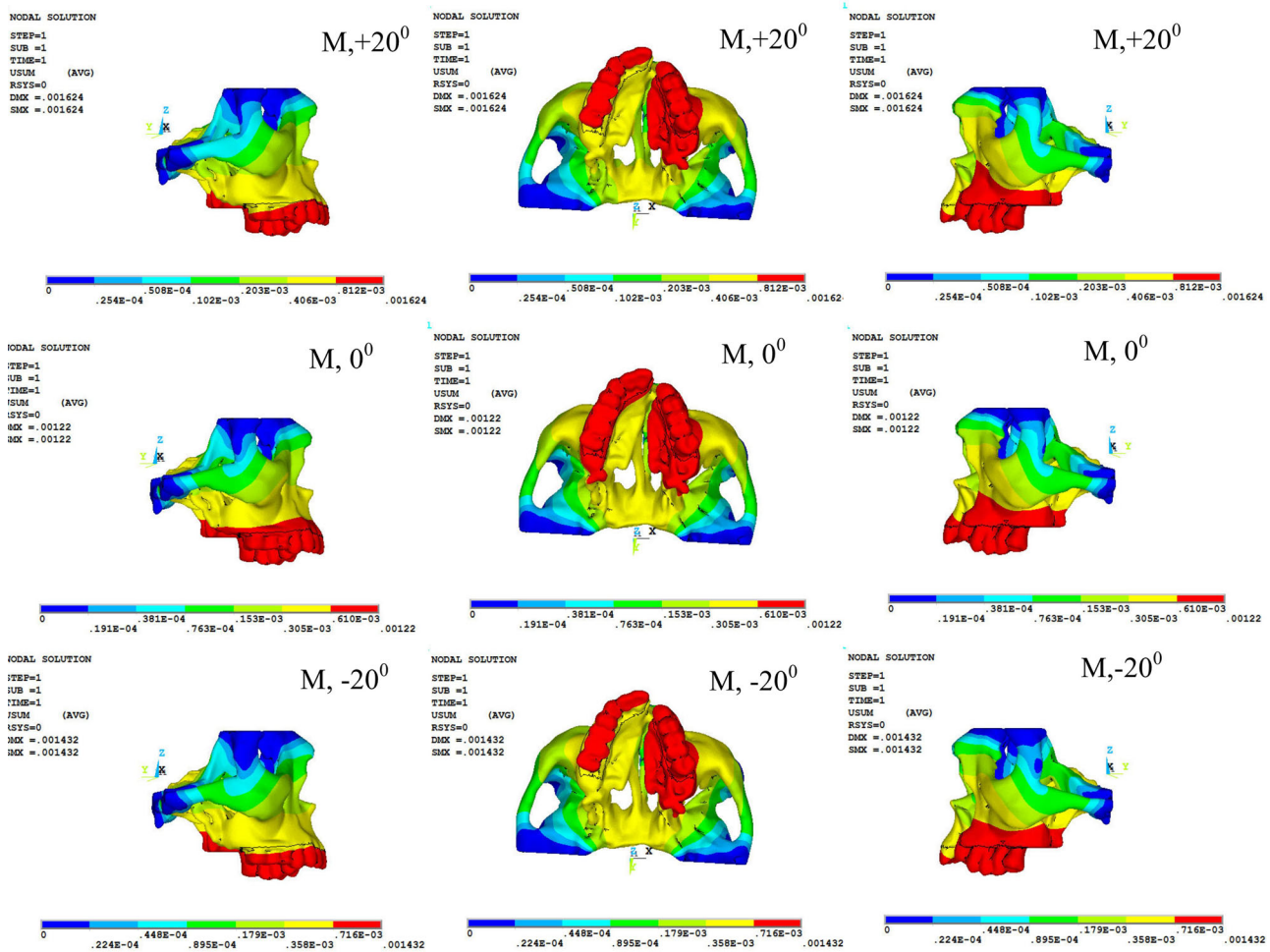
Figure 5. Initial displacement of craniofacial structures with only Maxgym forces.

were increased in protraction with expansion forces as compared to protraction-only forces (Figure 11). Expansion in the anterior region was slightly more as compared to expansion in the posterior region for protraction with expansion forces (Figure 11). MG produced greater transverse initial displacement than FM with and without expansion.

Analysis of initial displacement in sagittal direction (Y-axis)

The displacement of craniofacial structures in sagittal direction was more with protraction and expansion as compared to protraction only (Tables 2–5) (Figures 3, 5, 7, and 9). Dental structures displaced more as compared to skeletal structures, and initial displacement of structures on the cleft side was more as compared to noncleft side. MG produced greater sagittal displacement than FM with and without expansion. All skeletal nodes displaced forward except for orbit which displaced backward during protraction with and without expansion (Tables 2–5) (Figures 3, 5, 7,

and 9). Along Y-axis, the protraction forces at +20° produced more initial displacement both with and without expansion as compared to 0°, and −20°. The length of the palatal plane (PP), which is formed by a line joining ANS and PNS, increased more with only protraction forces as compared to protraction with expansion forces (Figure 12). The MG with and without expansion produced greater sagittal displacement than the FM.

Analysis of initial displacement in the vertical direction (Z-axis)

All skeletal nodes displaced upward except for right zygoma, central incisor crown, and subnasale which moved downward during protraction with and without expansion (Tables 2–5) (Figures 3, 5, 7, and 9). Dental structures displaced more than skeletal structures and dental structures. Cleft side produced greater initial displacement as compared to the noncleft side. The protraction forces at +20° produced more initial displacement as compared to 0°, and −20°.
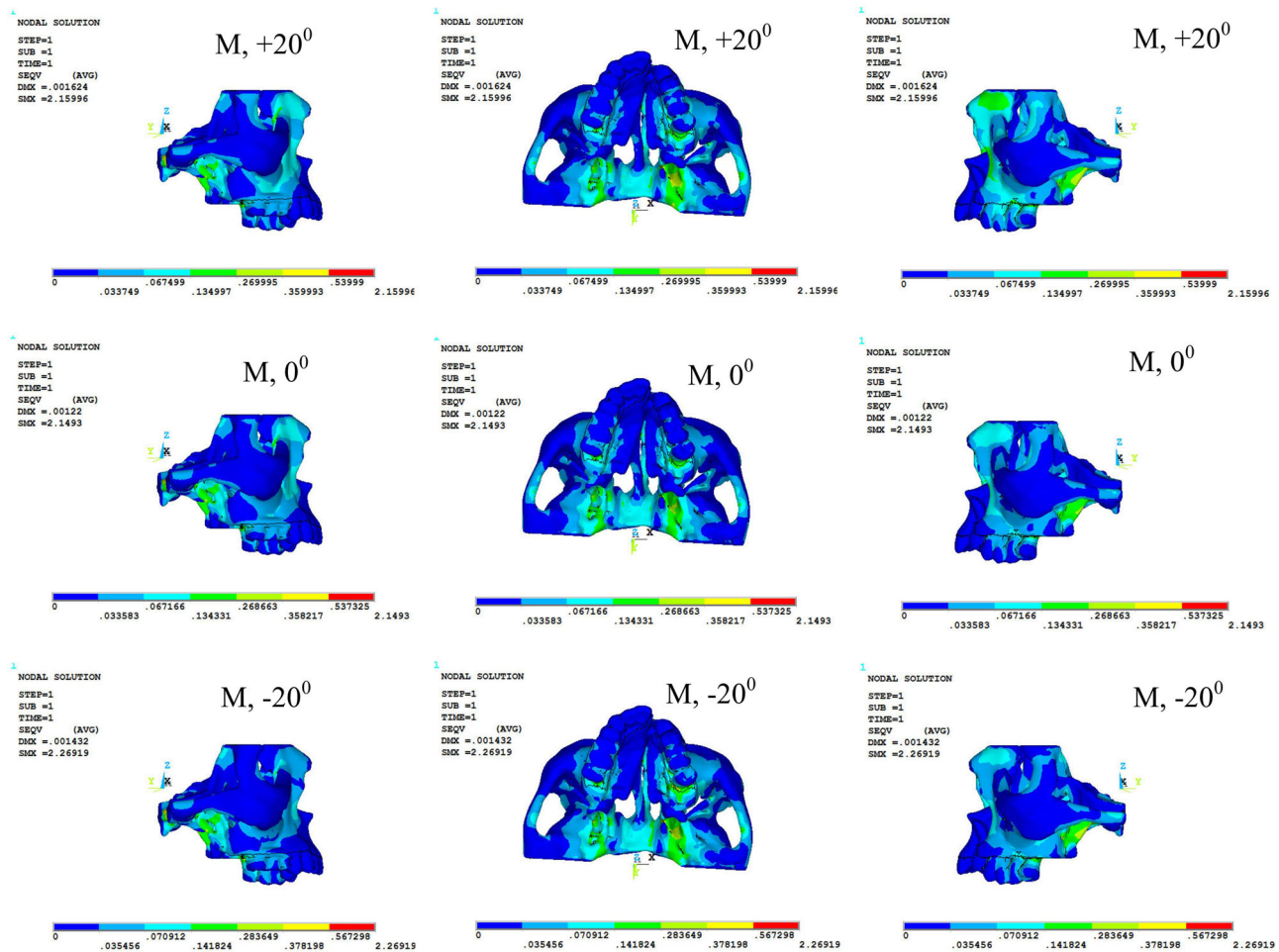
Figure 6. Distribution of stress on craniofacial structures with only Maxgym forces.

ANS moved upward in all angulations for both MG and FM forces with and without expansion (Figure 13). PNS moved upward for +20°, 0°, and downward for −20° for only protraction forces. However, PNS moved more upward in protraction with expansion forces as compared to protraction-only forces. CCW rotation of maxilla was observed less with protraction with expansion as compared to the only protraction. MG produced greater sagittal initial displacement than FM with and without expansion.

Von Mises stresses

Von Mises stresses were represented by SEQV (Tables 2–5) (Figures 4, 6, 8, and 10). A positive value indicated tensile stress and a negative value indicated compressive stress. With and without expansion, protraction forces at +20° produced the highest stress on all the structures followed by −20° and 0°. Higher stresses were recorded for protraction with expansion as compared to protraction-only forces. In the skeletal structures, higher von Mises stress was observed in zygoma, followed by orbit, PNS,

ANS, point A, and subnasale. In dental structures, higher stresses were observed on the noncleft side as compared to the cleft side. Stress generated on root apices was more than cusp tips and incisal edges.

Discussion

Maxillary deficiency in individuals with CLP due to surgical repair can be corrected with protraction with and without expansion. RME facilitates the correction of a mild midfacial deficiency by the forward displacement of the maxilla. Turley (1988) stated that palatal expansion disarticulates the maxilla and initiates cellular responses in these circummaxillary sutures allowing a more positive reaction to protraction forces. In this study, initial displacement of various craniofacial structures was considerably more during application of protraction with expansion forces as compared to protraction-only force (Tables 2–5). It was similar to results reported by several FEM studies (Gautam et al. 2009; Zhang et al. 2015).
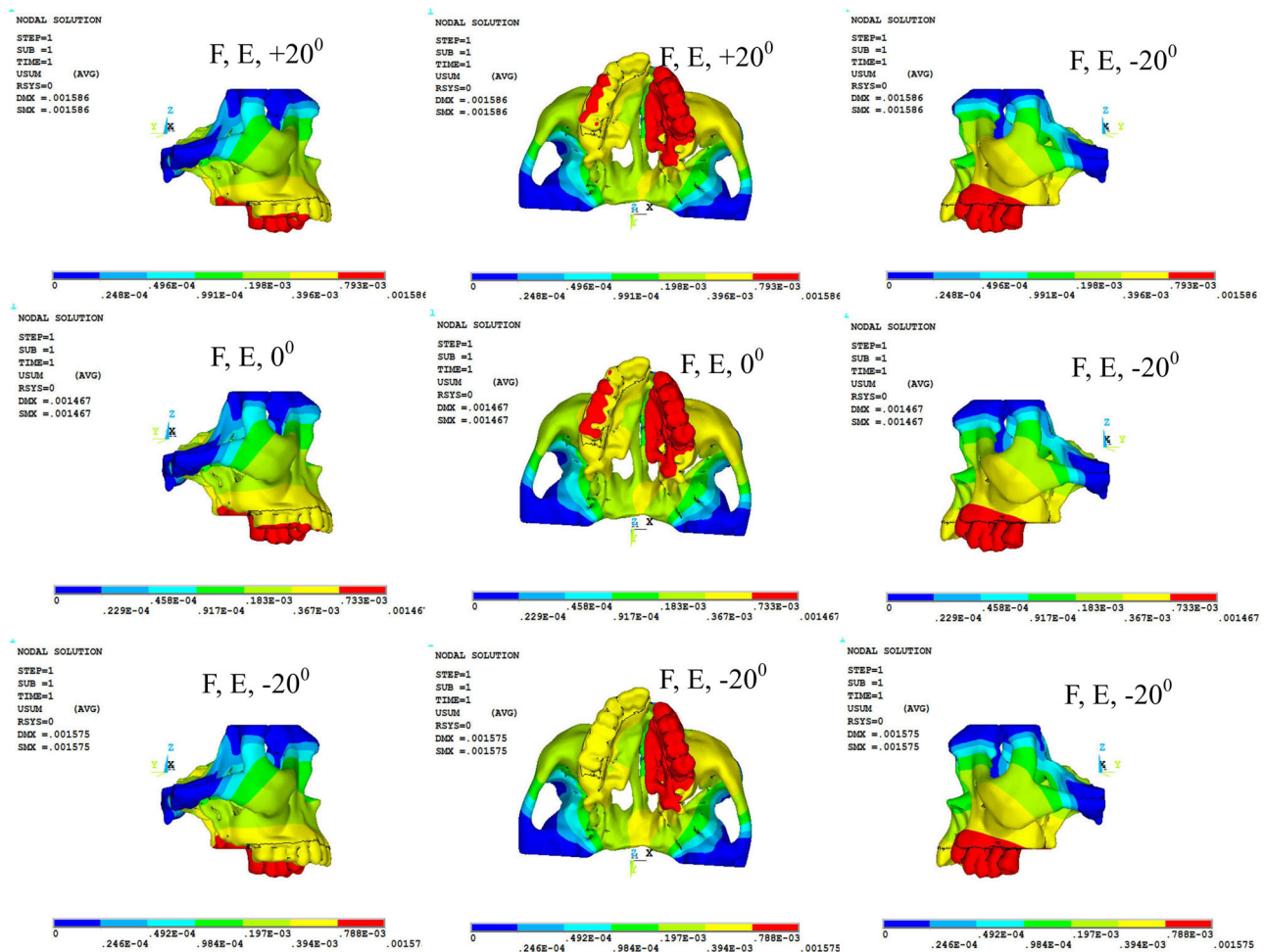
Figure 7. Initial displacement of craniofacial structures with facemask and expansion.

Chen et al. (2013) reported asymmetric protraction of maxilla in individuals with UCCLP when symmetric protraction forces are simulated. He iterated forces to achieve symmetric protraction which is advantageous and required in individuals with UCCLP (Chen et al. 2015). Yang et al. (2012) compared biomechanical effects of cleft types (UCCLP/BCCLP), protraction types (FM with RME and FM with miniplate), and models with and without alveolar bone grafting (ABG) using FEA. UCCLP model before ABG produced an asymmetric pattern of stress and initial displacement, which tended to be more symmetric after ABG (Yang et al. 2012). This study has also shown an asymmetric pattern of displacement on the cleft and noncleft sides of UCCLP when symmetrical protraction and expansion forces are applied (Tables 3 and 5).

Effect of amount of protraction forces on initial displacement

The optimal force in maxillary protraction therapy can be defined as the lowest force with the least duration that produced the greatest skeletal movement, and least dental movement counterclockwise (Yepes et al. 2014). A systematic review reported by him concluded that 300 g to 400 g per side is an optimal protraction force to bring about skeletal changes without causing any detrimental effects to the biological structures. Although heavy protraction forces simulated in an experimental model were of 500 g to 800 g, no conclusive data is available on the effects of heavy forces on craniofacial structures. In this study, the amount of initial displacement and distribution of stresses using MG protraction forces were kept at higher range as compared to FM protraction forces.

Effect of direction of protraction forces on palatal plane

During all loading conditions, ANS displaced more than PNS in the vertical direction, resulting in CCW of the palatal plane (Figure 13). The CCW rotation of palatal plane can be due to the differential movement of ANS and PNS and was observed in both, only protraction and protraction with expansion forces, which
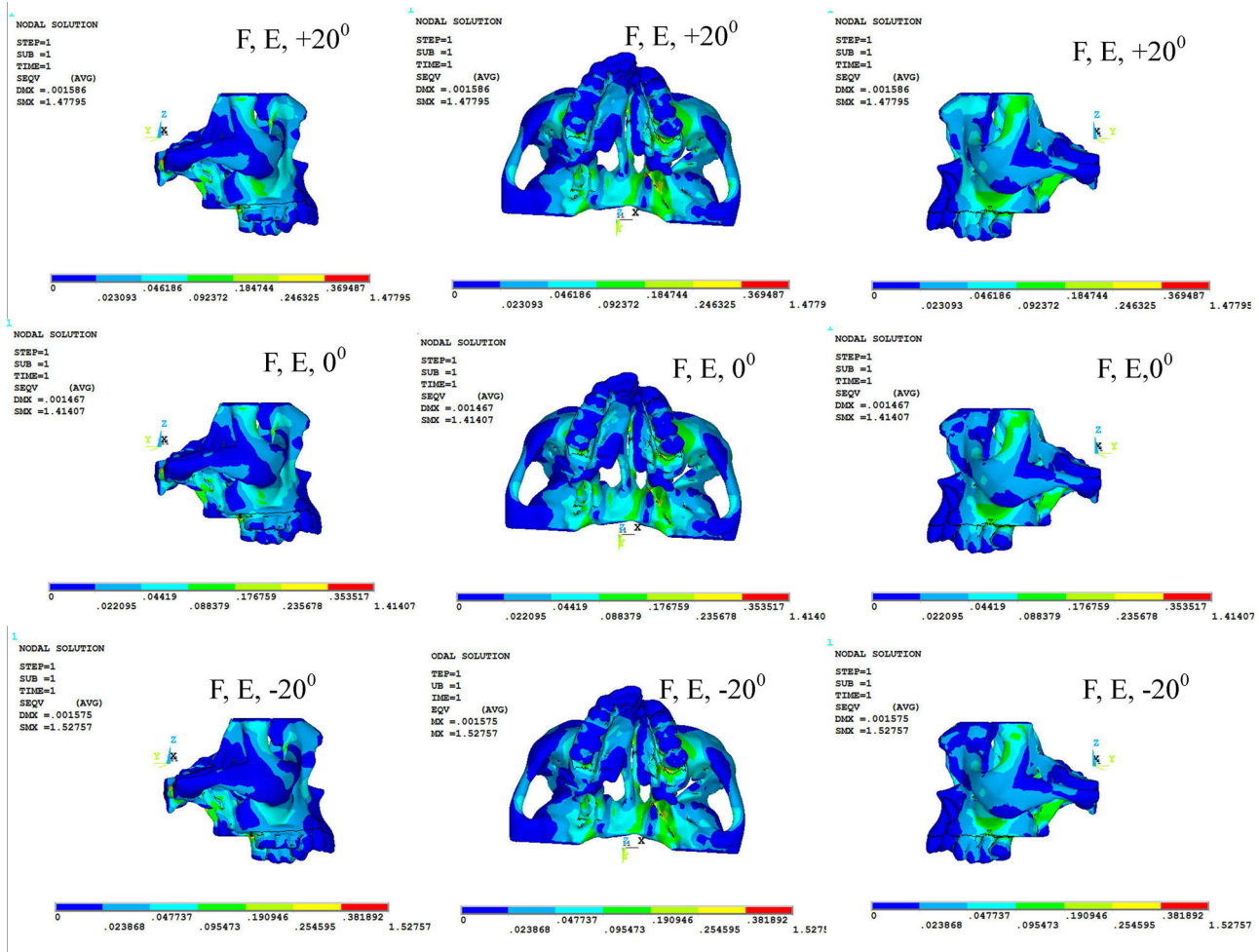
Figure 8. Distribution of stress on craniofacial structures with facemask and expansion.

is similar to the results obtained with earlier studies (Yan et al. 2013; Moon et al. 2015). The downward movement of PNS was noticed to only protraction forces at $-20°$ (Tables 2 and 3), and PNS moved upward when protraction supplemented with expansion (Tables 4 and 5). However, the displacement of PNS observed in both situations was very minimal as compared to the displacement of ANS. It was also observed that ANS moved less upward for simulation of protraction with expansion as compared to only protraction forces. Hence, counterclockwise rotation of the palatal plane was less for the simulation of protraction with expansion as compared to only protraction force.

The craniomaxillary complex displaced forward with a counterclockwise rotation, and the rotation degree decreased gradually with the increase of the angle between the force vector and occlusal plane (Yan et al. 2013). Similar results were also reported by Moon et al. 2015, where CCW rotation reduced with increased downward angulation between the

force vector and occlusal plane from $0°$ to $45°$. The maxillary displacement which was almost translatory or mild CCW at $-30°$ became CW at $-45°$. At $-30°$, the maxilla rotated in CCW to only protraction force, and the displacement became more translatory, when protraction along with expansion was simulated. The peak rotational amplitude and maximum protraction were observed at $-10°$ (Zhang et al. 2015).

Tanne et al. (1989) reported that $+45°$ to $+30°$ to the occlusal plane can produce most translatory repositioning of the craniofacial complex whereas $-30°$ downward force induced more uniform stress distribution to the craniofacial complex which is in accordance with our study.

Protraction with expansion, brought about increase in the width of the dental arch, increased considerably. The dental arch on the cleft side expanded more than on the noncleft side. This differential pattern of expansion would be suitable for patients with UCCLP. It has also been found in this study that the displacement of the dental arch increased gradually
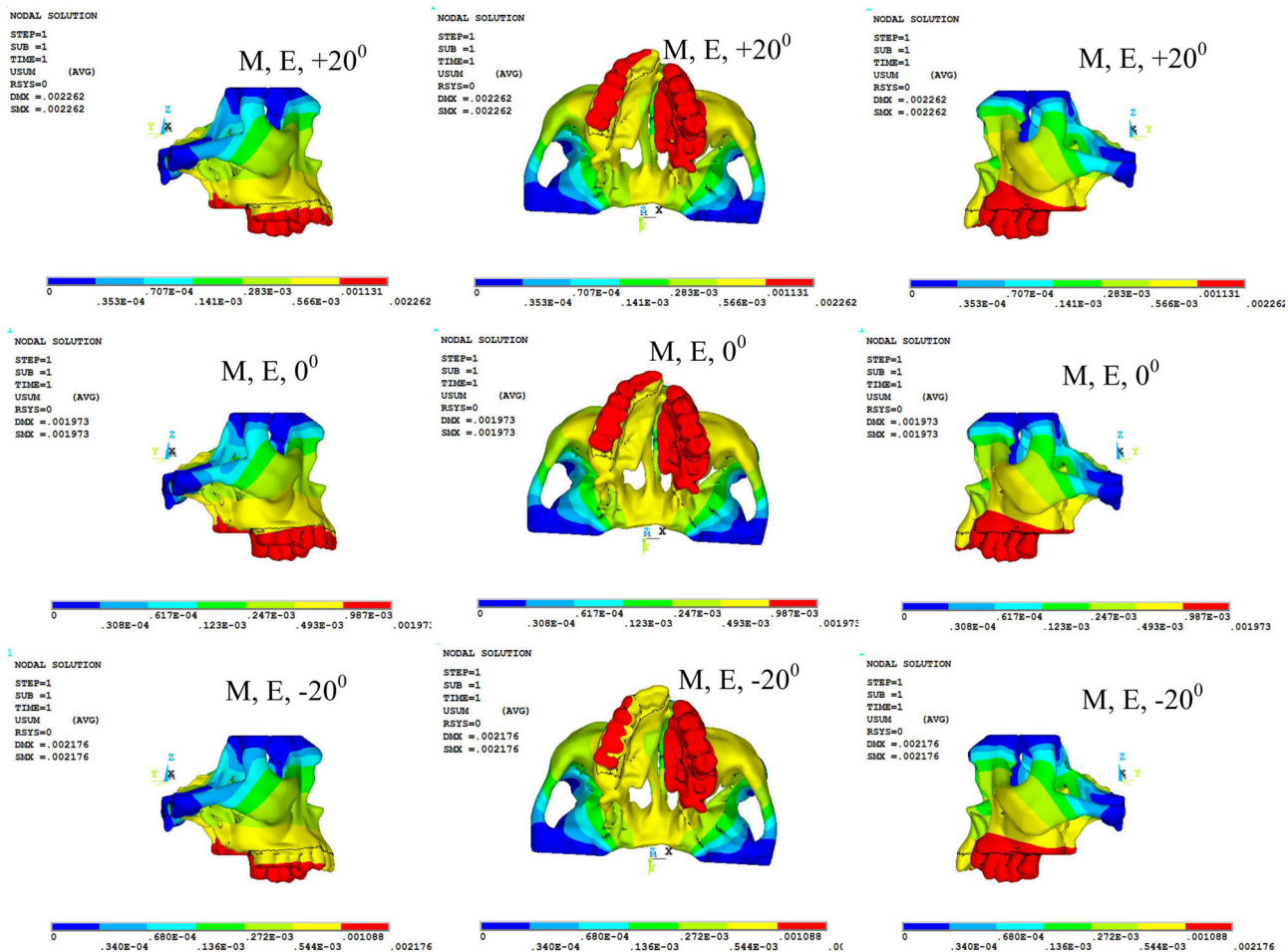
Figure 9. Initial displacement of craniofacial structures with Maxgym and expansion.

from posterior to anterior for the same degree of protraction (Figure 11).

Posterior movement of orbit for maxillary protraction therapy was unexpected and unexplained findings of this analysis and in contrary to the results reported by many researchers (Yang et al. 2012; Chen et al. 2013, 2015; Eom et al. 2018). The backward movement of orbit may be due to CCW movement of a palatal plane, resulting in tipping of maxilla superoposteriorly leading to a backward shift of orbit as it is superiorly placed.

Distribution of stress on craniofacial structures

In this study, the stresses generated on various craniofacial structures were evaluated using FE analysis. The structures articulated with other bones exhibited more stress than the structures on the extremities. Stress at the noncleft side is more as compared to that at the cleft side.

Limitation

The study has been carried out on virtual models, and it is based on a certain assumption. Although the results from this study give insight into the pattern of initial displacement and stress distribution during maxillary protraction using variable forces and direction, the real treatment outcome might vary due to the biological constraint.

Due to the limitations with the computational facility, only a part of the full skull was modeled. Hence, nodes around the foramen magnum and/or nodes located on the frontal and/or parietal bone are not fixed in this study. However, extreme ends of the FE model were fixed to produce a comparable effect for both treatment methods. In this study, a major focus was to compare the effectiveness of two treatment methods by analyzing the distribution of stresses and initial displacement generated in the vicinity of cleft, which is asymmetric. In order to standardize the application of fixed support, the
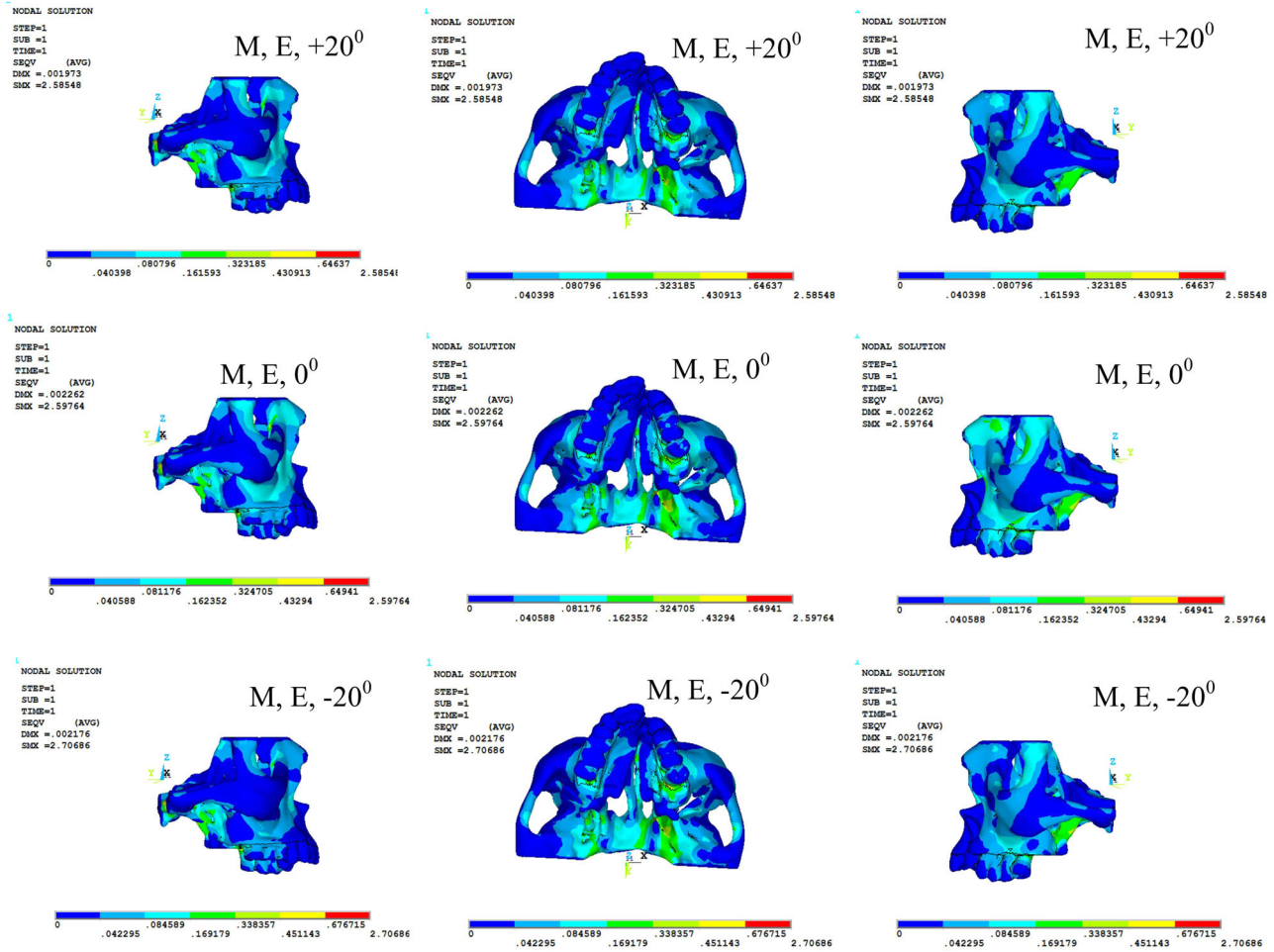
Figure 10. Distribution of stress on craniofacial structures for Maxgym and expansion.

comparison was made by maintaining the same location of boundary condition for both methods.

Conclusions

This study was conducted to investigate the effect of forces and angulations during application of two maxillary protraction forces (FM and MG) on the craniofacial structures in individuals with UCCLP with and without expansion.

The following conclusions are drawn from this study:

1. $+20^{\circ}$ protraction force produced maximum initial displacement in all the three X, Y, Z planes as compared to 0° or -20°.
2. In the transverse plane, protraction with expansion produced considerably more displacement than protraction only. The expansion in the anterior region was more as compared to expansion in the posterior region.
3. In the sagittal plane, the length of PP increased more with protraction only as compared to protraction with expansion.
4. In the vertical plane, CCW rotation of the maxilla occurred in all the instances. Protraction with expansion reduced upward displacement of ANS.
5. The craniofacial structures which are articulated with other bones exhibited more stress than the craniofacial structures on the extremities. $+20^{\circ}$ protraction produced more stress followed by -20° and 0°.
6. For all the situations, The MG produced greater initial displacement and stress as compared to FM.

Table 2. Initial displacement and stress on craniofacial structures along X, Y, Z planes for simulation of FM force at +20°, 0°, and −20° in a UCCLP model.

Sl. No.		F, +20°				F, 0°				F, −20°			
		X	Y	Z	SEQV	X	Y	Z	SEQV	X	Y	Z	SEQV
1.	Molar cusp (NC)	−1.30E-04 (L)	−3.94E-04 (F)	+8.36E-05 (U)	+1.45E-02	−1.02E-04 (L)	−3.68E-04 (F)	+5.23E-05 (U)	+1.37E-02	−8.53E-05 (L)	−3.67E-04 (F)	+2.21E-05 (U)	+1.47E-02
2.	Molar root (NC)	+1.23E-04 (M)	−3.78E-04 (F)	+7.73E-05 (U)	+2.71E-02	+1.07E-0 (M)	−2.68E-04 (F)	+2.13E-05 (U)	+1.72E-02	+1.44E-04 (M)	−3.32E-04 (F)	−1.34E-05 (D)	+2.41E-02
3.	PM cusp (NC)	−1.27E-04 (L)	−4.25E-04 (F)	+1.99E-04 (U)	+2.36E-03	−9.34E-05 (L)	−3.98E-04 (F)	+1.62E-04 (U)	+1.99E-03	−6.92E-05 (L)	−3.99E-04 (F)	+1.31E-04 (U)	+1.89E-03
4.	PM root (NC)	−4.86E-05 (L)	−2.30E-04 (F)	+1.78E-04 (U)	+2.33E-02	−3.45E-05 (L)	−2.12E-04 (F)	+1.44E-04 (U)	+1.88E-02	−2.76E-05 (L)	−2.12E-04 (F)	+1.17E-04 (U)	+1.42E-02
5.	Canine (NC)	−1.13E-04 (L)	−4.14E-04 (F)	+2.32E-04 (U)	+2.23E-03	−8.10E-05 (L)	−3.88E-04 (F)	+1.92E-04 (U)	+1.86E-03	−5.78E-05 (L)	−3.88E-04 (F)	+1.61E-04 (U)	+1.64E-03
6.	CI crown (NC)	−8.76E-05 (L)	−3.72E-04 (F)	+2.37E-04 (U)	+4.94E-04	−5.52E-05 (L)	−3.44E-04 (F)	+2.12E-04 (U)	+4.39E-04	−3.05E-05 (L)	−3.40E-04 (F)	+1.98E-04 (U)	+3.71E-04
7.	CI root (NC)	+1.17E-04 (M)	−5.83E-04 (F)	+3.88E-04 (U)	+1.61E-03	+1.10E-04 (M)	−4.14E-04 (F)	+2.32E-04 (U)	+8.35E-04	+1.50E-04 (M)	−5.14E-04 (F)	+2.41E-04 (U)	+7.56E-04
8.	Zygoma (NC)	+6.33E-05 (M)	−1.13E-04 (F)	−1.61E-04 (D)	+4.18E-02	+5.65E-05 (M)	−8.22E-05 (F)	−1.46E-04 (D)	+3.02E-02	+7.18E-05 (M)	−9.86E-05 (F)	−1.97E-04 (D)	+3.72E-02
9.	Orbit (NC)	−9.95E-06 (L)	+5.05E-06 (B)	+1.27E-05 (U)	+2.42E-02	−5.70E-06 (L)	+3.01E-06 (B)	+7.99E-06 (U)	+1.63E-02	−1.07E-06 (L)	+1.87E-06 (B)	+3.56E-06 (U)	+1.00E-02
10.	Nasal bone	−4.32E-06 (NC)	−2.20E-05 (F)	+4.79E-05 (U)	+1.27E-02	−2.84E-06 (NC)	−1.55E-05 (F)	+3.47E-05 (U)	+7.93E-03	−2.00E-06 (NC)	−1.31E-05 (F)	+3.00E-05 (U)	+7.13E-03
11.	Subnasale	−8.35E-05 (NC)	−1.74E-04 (F)	−8.09E-05 (D)	+6.84E-03	−7.49E-05 (D)	−1.58E-04 (F)	−8.80E-05 (D)	+6.89E-03	−7.58E-05 (NC)	−1.59E-04 (F)	−1.10E-04 (D)	+6.06E-03
12.	Point A	−1.60E-05 (NC)	−1.55E-04 (F)	+1.88E-04 (U)	+2.59E-03	−4.86E-06 (NC)	−1.39E-04 (F)	+1.67E-04 (U)	+1.03E-03	+9.45E-07 (C)	−1.37E-04 (F)	+1.55E-04 (U)	+6.23E-04
13.	ANS	+1.68E-05 (C)	−7.07E-05 (F)	+2.10E-04 (U)	+7.01E-05	+1.99E-05 (C)	−6.21E-05 (F)	+1.87E-04 (U)	+7.29E-05	+1.94E-05 (C)	−6.03E-05 (F)	+1.74E-04 (U)	+1.11E-04
14.	PNS	−2.28E-05 (NC)	−9.88E-05 (F)	+9.12E-06 (U)	+1.53E-02	−1.23E-05 (NC)	−8.63E-05 (F)	+2.08E-06 (U)	+1.37E-02	−5.16E-06 (NC)	−8.14E-05 (F)	−4.11E-06 (D)	+1.31E-02
15.	Orbit (C)	+4.10E-05 (L)	+1.95E-5 (B)	+2.46E-05 (U)	+2.01E-02	+2.28E-05 (L)	+9.97E-05 (B)	+1.46E-05 (U)	+1.29E-02	+2.10E-05 (L)	4.86E-06 (B)	+1.29E-05 (U)	+1.26E-02
16.	Zygoma (C)	+1.83E-04 (L)	−1.65E-04 (F)	+1.25E-04 (U)	+5.01E-02	+1.16E-04 (L)	−1.02E-04 (F)	+6.40E-05 (U)	+2.19E-02	+1.27E-04 (L)	−1.13E-04 (F)	+5.12E-05 (U)	+1.26E-02
17.	CI root (C)	+1.53E-04 (L)	−3.73E-04 (F)	+2.84E-04 (U)	+4.72E-02	+1.16E-04 (L)	−2.57E-04 (F)	+1.68E-04 (U)	+2.74E-02	+1.46E-04 (L)	−3.11E-04 (F)	+1.67E-04 (U)	+2.70E-02
18.	CI crown (C)	−9.67E-05 (M)	−1.88E-04 (F)	−1.35E-04 (D)	+345E-02	−8.90E-05 (M)	−1.75E-04 (F)	−1.41E-04 (D)	+3.53E-02	−9.50E-05 (M)	−1.77E-04 (F)	−1.64E-04 (D)	+3.23E-02
19.	Canine (C)	+1.14E-04 (L)	−5.87E-04 (F)	+4.25E-04 (U)	+1.84E-03	+1.06E-04 (L)	−4.18E-04 (F)	+2.67E-04 (U)	+1.32E-03	+1.45E-04 (L)	−5.20E-04 (F)	+2.90E-04 (U)	+1.74E-03
20.	PM root (C)	+1.58E-04 (L)	−3.70E-04 (F)	+2.23E-04 (U)	+5.60E-02	+1.21E-04 (L)	−2.56E-04 (F)	+1.24E-04 (U)	+3.09E-02	+1.52E-04 (L)	−3.12E-04 (F)	+1.13E-04 (U)	+2.78E-02
21.	PM cusp (C)	+1.24E-04 (L)	−6.82E-04 (F)	+3.52E-04 (U)	+1.08E-03	+1.21E-04 (L)	−4.92E-04 (F)	+2.12E-04 (U)	+7.24E-04	+1.69E-04 (L)	−6.17E-04 (F)	+2.20E-04 (U)	+1.04E-03
22.	Molar root (C)	+1.41E-04(L)	−3.53E-04 (F)	+1.07E-04 (U)	+1.31E-02	+1.13E-04 (L)	−2.48E-04 (F)	+4.10E-05 (U)	+5.89E-03	+1.45E-04 (L)	−3.04E-04 (F)	+9.01E-06 (U)	+8.19E-03
23.	Molar cusp (C)	+1.40E-04 (L)	−7.07E-04 (F)	+1.67E-04 (U)	+1.37E-02	+1.38E-04 (L)	−5.09E-04 (F)	+6.56E-05 (U)	+1.01E-02	+1.93E-04 (L)	−6.40E-04 (F)	+2.30E-04 (U)	+1.47E-02

Analysis was carried out using ANSYS 19; Inc., Canonsburg, PA. Displacement was measured in mm. Stress was measured in N/mm.² M (600 g/side) represented MG force. Along X-axis, cleft side: negative value indicated medial movement (M), and positive value indicated lateral movement (L), Noncleft side: Positive value indicated medial movement (M), and negative value indicated lateral movement (L). Midline structures: negative value indicated noncleft movement (NC), and positive value indicated cleft side movement (C). Along Y-axis: negative value indicated forward movement (F), and positive value indicated backward movement (B). Along Z-axis: negative value indicated downward movement (D), and positive value indicated upward movement (U), von Mises stress (=SEQV): negative value indicated compressive stress, and positive value indicated tensile stress. Abbreviations used: MG: Maxgym; C: cleft, NC: noncleft, ANS: anterior nasal spine, PM: premolar, CI: center incisor.

Table 3. Initial displacement and stress on craniofacial structures along X, Y, Z planes for simulation of MG force at +20°, 0°, and −20° in a UCCLP model.

Sl. No.	Variables	M, +20°				M, 0°				M, −20°			
		X	Y	Z	SEQV	X	Y	Z	SEQV	X	Y	Z	SEQV
1.	Molar cusp (NC)	−2.72E-4 (L)	−8.22E-04 (F)	+1.78E-04 (U)	+3.05E-02	−2.24E-04 (L)	−8.10E-04 (F)	+1.15E-04 (U)	+3.02E-02	−1.75E-04 (L)	−7.62E-04 (F)	+4.24E-05 (U)	+3.09E-02
2.	Molar root (NC)	+2.55E-04 (M)	−7.88E-04 (F)	+1.66E-04 (U)	+5.73E-02	+2.36E-04 (M)	−5.91E-04 (F)	+4.69E-05 (U)	+3.78E-02	+3.01E-04 (M)	−6.88E-04 (F)	−3.32E-05 (D)	+5.06E-02
3.	PM cusp (NC)	−2.68E-04 (L)	−8.86E-04 (F)	+4.18E-04 (U)	+4.96E-03	−2.06E-04 (L)	−8.76E-04 (F)	+3.55E-04 (U)	+4.39E-03	−1.41E-04 (L)	−8.28E-04 (F)	+2.69E-04 (U)	+3.94E-03
4.	PM root (NC)	−1.02E-04 (L)	−4.79E-04 (F)	+3.75E-04 (U)	+4.91E-02	−7.60E-05 (L)	−4.67E-04 (F)	+3.17E-04 (U)	+4.14E-02	−5.62E-05 (L)	−4.40E-04 (F)	+2.69E-04 (U)	+2.90E-02
5.	Canine (NC)	−2.38E-04 (L)	−8.63E-04 (F)	+4.87E-04 (U)	+4.68E-03	−1.78E-04 (L)	−8.53E-04 (F)	+4.23E-04 (U)	+4.09E-03	−1.17E-04 (L)	−8.06E-04 (F)	+3.31E-04 (U)	+3.39E-03
6.	CI crown (NC)	−1.86E-04 (L)	−7.77E-04 (F)	+4.96E-04 (U)	+1.03E-03	−1.22E-04 (L)	−7.56E-04 (F)	+4.66E-04 (U)	+9.66E-04	−5.99E-05 (L)	−7.06E-04 (F)	+4.09E-04 (U)	+7.66E-04
7.	CI root (NC)	+2.42E-04 (M)	−1.22E-03 (F)	+8.17E-04 (U)	+3.42E-03	+2.41E-04 (M)	−9.12E-04 (F)	+5.10E-04 (U)	+1.84E-03	+3.15E-04 (M)	−1.07E-03 (F)	+4.92E-04 (U)	+1.54E-03
8.	Zygoma (NC)	+1.31E-04 (M)	−2.37E-04 (F)	−3.33E-04 (D)	+8.72E-02	+1.24E-04 (M)	−1.81E-04 (F)	−3.20E-04 (D)	+6.65E-02	+1.50E-04 (M)	−2.04E-04 (F)	−4.12E-04 (D)	+7.71E-02
9.	Orbit (NC)	−2.12E-05 (L)	+1.07E05 (B)	+2.69E-05 (U)	+5.12E-02	−1.25E-05 (L)	+6.62E06 (B)	+1.76E-05 (U)	+3.58E-02	−1.69E-06 (L)	+3.71E06 (B)	+6.87E-06 (U)	+2.00E-02
10.	Nasal bone	−9.13E-06 (NC)	−4.62E-05 (F)	+1.01E-04 (U)	+2.67E-02	−6.24E-06 (Lt)	−3.40E-05 (F)	+7.63E-05 (U)	+1.74E-02	−4.03E-06 (NC)	−2.66E-05 (F)	+6.14E-05 (U)	+1.45E-02
11.	Subnasale	−1.74E-04 (NC)	−3.62E-04 (F)	−1.67E-04 (D)	+1.43E-02	−1.65E-04 (Lt)	−3.48E-04 (F)	−1.94E-04 (D)	+1.52E-02	−1.57E-04 (NC)	−3.31E-04 (F)	−2.30E-04 (U)	+1.26E-02
12.	Point A	−3.43E-05 (NC)	−3.23E-04 (F)	+3.94E-04 (U)	+5.52E-03	−1.07E-05 (Lt)	−3.07E-04 (F)	+3.67E-04 (U)	+2.27E-03	+2.98E-06 (C)	−2.83E-04 (F)	+3.20E-04 (U)	+1.30E-03
13.	ANS	+3.47E-05 (C)	−1.48E-04 (F)	+4.40E-04 (U)	+1.48E-04	4.37E-05 (Rt)	−1.37E-04 (F)	+4.10E-04 (U)	+1.60E-04	+4.05E-05 (C)	−1.25E-04 (F)	+3.59E-04 (U)	+2.37E-04
14.	PNS	−4.84E-05 (NC)	−2.07E-04 (F)	+1.98E-05 (U)	+3.20E-02	−2.70E-05 (Rt)	−1.90E-04 (F)	+4.58E-06 (U)	+3.00E-02	−9.69E-06 (NC)	−1.68E-04 (F)	−9.35E-06 (D)	+2.72E-02
15.	Orbit (C)	+8.66E-05 (L)	+4.14E05 (B)	+5.20E-05 (U)	+4.22E-02	+5.01E-05 (L)	+2.19E05 (B)	+3.21E-05 (U)	+2.83E-02	+4.26E-05 (L)	+9.24E06 (B)	+2.61E-05 (U)	+2.58E-02
16.	Zygoma (C)	+3.83E-04 (L)	−3.46E-04 (F)	+2.64E-04 (U)	+0.10642	+2.55E-04 (L)	−2.25E-04 (F)	+1.41E-04 (U)	+4.82E-02	+2.60E-04 (L)	−2.31E-04 (F)	+1.02E-04 (U)	+2.39E-02
17.	CI root (C)	+3.18E-04 (L)	−7.80E-04 (F)	+5.98E-04 (U)	+9.93E-02	+2.56E-04 (L)	−5.66E-04 (F)	+3.69E-04 (U)	+6.02E-02	+3.03E-04 (L)	−6.44E-04 (F)	+3.41E-04 (U)	+5.50E-02
18.	CI crown (C)	−2.01E-04 (M)	−3.92E-04 (F)	−2.80E-04 (D)	+7.19E-02	−1.96E-04 (M)	−3.84E-04 (F)	−3.11E-04 (D)	+7.77E-02	−1.97E-04 (M)	−3.68E-04 (F)	−3.42E-04 (D)	+6.70E-02
19.	Canine (C)	+2.35E-04 (L)	−1.23E-03 (F)	+8.92E-04 (U)	+3.84E-03	+2.33E-04 (L)	−9.20E-04 (F)	+5.87E-04 (U)	+2.91E-03	+3.04E-04 (L)	−1.08E-03 (F)	5.96E-04 (U)	+3.63E-03
20.	PM root (C)	+3.28E-04 (L)	−7.73E-04 (F)	+4.70E-04 (U)	+0.11828	+2.66E-04 (L)	−5.64E-04 (F)	+2.72E-04 (U)	+6.79E-02	+3.16E-04 (L)	−6.45E-04 (F)	+2.28E-04 (U)	+5.61E-02
21.	PM cusp (C)	+2.54E-04 (L)	−1.42E-03 (F)	+7.41E-04 (U)	+2.27E-03	+2.66E-04 (L)	−1.08E-03 (F)	+4.67E-04 (U)	+1.59E-03	+3.54E-04 (L)	−1.28E-03 (F)	+4.49E-04 (U)	+2.17E-03
22.	Molar root (C)	+2.93E-04 (L)	−7.37E-04 (F)	+2.29E-04 (U)	+2.81E-02	+2.48E-04 (L)	−5.45E-04 (F)	+9.01E-05 (U)	+1.30E-02	+3.01E-04 (L)	−6.30E-04 (F)	+1.29E-05 (U)	+1.74E-02
23.	Molar cusp (C)	+2.88E-04 (L)	−1.47E-03 (F)	+3.56E-04 (U)	+2.85E-02	+3.03E-04 (F)	−1.12E-03 (F)	+1.44E-04 (U)	+2.21E-02	+4.04E-04 (L)	−1.33E-03 (F)	+3.93E-05 (U)	+3.08E-02

Analysis was carried out using ANSYS 19; Inc., Canonsburg, PA. Displacement was measured in mm. Stress was measured in N/mm.² M (600 g/side) represented MG force. Along X-axis, cleft side: negative value indicated medial movement (M), and positive value indicated lateral movement (L), noncleft side: positive value indicated medial movement (M), and negative value indicated lateral movement (L). Midline structures: negative value indicated noncleft movement (NC), and positive value indicated cleft side movement (C). Along Y-axis: negative value indicated forward movement (F), and positive value indicated backward movement (B). Along Z-axis: negative value indicated downward movement (D), and positive value indicated upward movement (U), von Mises stress (=SEQV): negative value indicated compressive stress, and positive value indicated tensile stress. Abbreviations used: MG-Maxgym, C: cleft, NC: noncleft, ANS: anterior nasal spine, PM: premolar, CI: center incisor.

Table 4. Initial displacement and stress on craniofacial structures along X, Y, Z planes for simulation of FM and RME forces at $+20°$, $0°$, and $−20°$ in a UCCLP model.

Sl. No.	Variables	F, E, +20°				F, E, 0°				F, E, −20°			
		X	Y	Z	SEQV	X	Y	Z	SEQV	X	Y	Z	SEQV
1.	Molar cusp (NC)	−5.29E−04 (L)	−5.24E−04 (F)	+9.12E−05 (U)	+1.24E−02	−5.01E−04 (L)	−4.98E−04 (F)	+5.99E−05 (U)	+1.34E−02	−4.84E−04 (L)	−4.97E−04 (F)	+2.97E−05(U)	+1.60E−02
2.	Molar root (NC)	+5.85E04 (M)	−3.81E−04 (F)	+1.36E−04 (U)	+0.14394	+5.69E04 (M)	−2.72E−04 (F)	+8.00E−05 (U)	+0.13387	+6.06E04 (M)	−3.35E−04 (F)	+4.53E−05(D)	+0.12148
3.	PM cusp (NC)	−5.15E−04 (L)	−5.77E−04 (F)	+3.14E−04 (U)	+1.18E−02	−4.82E−04 (L)	−5.50E−04 (F)	+2.76E−04 (U)	+1.13E−02	−4.58E−04 (L)	−5.51E−04 (F)	+2.46E−04(U)	+1.10E−02
4.	PM root (NC)	−2.48E−04 (L)	−2.80E−04 (F)	+2.75E−04 (U)	+3.71E−02	−2.34E−04 (L)	−2.63E−04 (F)	+2.41E−04 (U)	+3.27E−02	−2.27E−04 (L)	−2.62E−04 (F)	+2.13E−04 (U)	+2.81E−02
5.	Canine (NC)	−4.75E−04 (L)	−5.63E−04 (F)	+3.75E−04 (U)	+7.01E−03	−4.43E−04 (L)	−5.37E−04 (F)	+3.35E−04 (U)	+6.77E−03	−4.20E−04 (L)	−5.37E−04 (F)	+3.04E−04 (U)	+6.61E−03
6.	CI crown (NC)	−4.23E−04 (L)	−4.70E−04 (F)	+2.50E−04 (U)	+1.28E−03	−3.91E−04 (L)	−4.41E−04 (F)	+2.25E−04 (U)	+1.23E−03	−3.66E−04 (L)	−4.37E−04 (F)	+2.11E−04 (U)	+1.16E−03
7.	CI root (NC)	+1.07E03 (M)	−7.32E−04 (F)	+1.52E−04 (U)	+5.80E−03	+1.06E03 (M)	−5.63E−04 (F)	−4.36E−06 (U)	+5.01E−03	+1.10E03 (M)	−6.63E−04 (F)	+4.53E−06 (U)	+4.77E−03
8.	Zygoma (NC)	+1.41E04 (M)	−1.42E−04 (M)	−2.92E−04 (D)	+4.98E−02	+1.34E04 (M)	−1.11E−04 (M)	−2.77E−04 (D)	+3.97E−02	1.49E−04 (M)	−1.27E−04 (M)	−3.28E−05 (U)	+4.73E−02
9.	Orbit (NC)	−3.78E−05 (Lt)	+1.95E−05 (B)	+4.19E−05 (U)	+7.44E−02	−3.36E−05 (L)	+1.75E−05 (B)	+3.73E−05 (U)	+6.64E−02	−2.89E−05 (L)	+1.63E−05 (B)	+3.29E−05 (U)	+6.01E−02
10.	Nasal bone	+7.32E06 (Lt)	−6.41E−06 (F)	+2.05E−05 (U)	+1.39E−02	+8.80E06 (Lt)	+7.76E−08 (F)	+7.31E−06 (U)	+1.12E−02	+9.64E06 (Lt)	+2.48E−06 (F)	+2.65E−06 (U)	+1.01E−02
11.	Subnasale	−2.60E−04 (Rt)	−2.17E−04 (F)	−1.98E−04 (D)	+2.39E−02	−2.52E−04 (Lt)	−2.01E−04 (F)	−2.05E−04 (D)	+2.41E−02	−2.53E−04 (Lt)	−2.02E−04 (F)	−2.27E−04 (D)	+2.38E−02
12.	Point A	−1.90E−04 (Lt)	−1.76E−04 (F)	+1.70E−04 (U)	+4.11E−03	−1.79E−04 (Lt)	−1.60E−04 (F)	+1.49E−04 (U)	+3.64E−03	−1.73E−04 (Rt)	−1.57E−04 (F)	+1.36E−04 (U)	+3.49E−03
13.	ANS	−9.77E−05 (Rt)	−7.02E−05 (F)	+1.96E−04 (U)	+6.02E−04	−9.46E−05 (Rt)	−6.16E−05 (F)	+1.73E−04 (U)	+6.53E−04	−9.51E−05 (Rt)	−5.98E−05 (F)	+1.60E−04 (U)	+7.04E−04
14.	PNS	−1.70E−04 (Lt)	−1.66E−04 (F)	+6.44E−05 (U)	+2.15E−02	−1.59E−04 (Rt)	−1.53E−04 (F)	+5.74E−05 (U)	+1.98E−02	−1.52E−04 (Lt)	−1.48E−04 (F)	+5.12E−05 (D)	+1.93E−02
15.	Orbit (C)	+1.55E−04 (L)	+8.07E−05 (B)	+1.07E−04 (U)	+6.88E−02	+1.37E−05 (B)	+7.12E−05 (B)	+1.75E−05 (U)	+6.27E−02	+1.35E−04 (L)	+6.61E−05 (B)	+9.49E−05 (U)	+6.22E−02
16.	Zygoma (C)	+3.13E−04 (L)	−1.19E−04 (F)	+7.84E−05 (U)	+1.08E−02	+2.46E−04 (L)	−5.62E−04 (F)	+1.75E−05 (U)	+3.61E−02	+2.57E−04 (L)	−6.66E−04 (F)	+4.74E−06 (U)	+4.53E−02
17.	CI root (C)	+6.36E−04 (L)	−3.91E−04 (F)	+2.80E−04 (U)	+5.05E−02	+5.99E−04 (L)	−2.75E−04 (F)	+1.64E−04(U)	+3.18E−02	+6.29E−04(L)	−3.29E−04 (F)	+1.63E−04 (U)	+3.19E−02
18.	CI crown (C)	−2.55E−04 (M)	−2.38E−04 (F)	−2.09E−04 (D)	+7.64E−02	−2.48E−04 (M)	−2.25E−04 (F)	−2.15E−04 (D)	+7.72E−02	−2.54E−04(M)	−2.27E−04 (F)	−2.37E−04 (D)	+7.38E−02
19.	Canine (C)	+1.07E−03 (L)	−7.06E−04 (F)	+3.68E−04 (U)	+4.06E−03	+1.06E−03 (L)	−5.37E−04 (F)	+2.09E−04 (U)	+3.55E−03	+1.10E−03(L)	−6.39E−04 (F)	+2.33E−04(U)	+3.97E−03
20.	PM root (C)	+6.14E−04 (L)	−3.77E−04 (F)	+2.41E−04(U)	+7.62E−02	+5.77E−04 (L)	−2.63E−04 (F)	+1.42E−04 (U)	+5.74E−02	+6.09E−04(L)	−3.19E−04 (F)	+1.31E−04 (U)	+5.53E−02
21.	PM cusp (C)	+1.25E−03 (L)	−8.32E−04 (F)	+3.12E−04(D)	+3.04E−03	+1.25E−03 (L)	−6.42E−04 (F)	+1.72E−04 (U)	+2.64E−03	+1.30E−03(L)	−7.68E−04 (F)	+1.80E−04 (U)	+2.70E−03
22.	Molar root (C)	+5.54E−04 (L)	−3.50E−04 (L)	+1.55E−04(U)	+5.01E−02	+5.25E−04 (L)	−2.45E−04 (L)	+8.85E−05 (U)	+4.80E−02	+5.57E−04(L)	−3.02E−04 (F)	+5.66E−05 (U)	+4.48E−02
23.	Molar cusp (C)	+1.24E−03 (L)	−8.83E−04 (F)	−3.41E−05 (U)	+1.34E−02	+1.24E−03 (L)	−6.86E−04 (F)	−1.35E−04 (U)	+1.12E−02	+1.30E−03 (L)	−8.17E−04 (F)	−1.78E−04 (F)	+1.60E−02

Analysis was carried out using ANSYS 19; Inc., Canonsburg, PA. Initial displacement was measured in mm. Stress was measured in N/mm². F (300 g/side) represented FM force, E (500 g) represented RME force. Abbreviations used: FM: facemask, RME: rapid maxillary expansion, C: cleft, NC: noncleft, ANS: anterior nasal spine, PM: premolar, CI: center incisor. Along X-axis, cleft side: negative value indicated medial movement (M) and positive value indicated lateral movement (L), noncleft side: positive value indicated medial movement (M) and negative value indicated lateral movement (L). Midline structures: negative value indicated noncleft movement (NC) and positive value indicated cleft side movement (C). Along Y-axis: negative value indicated forward movement (F) and positive value indicated backward movement (B). Along Z-axis: negative value indicated downward movement (D) and positive value indicated upward movement (U), von Mises stress (SEQV): negative sign indicated compressive stress and positive sign indicated tensile stress.

Table 5. Displacement and stress on craniofacial structures along X, Y, Z planes for simulation of MG and SME force at +20°, 0°, and −20° in a UCCLP model.

Sl. No.	Variables	M, E1, +20°				M, E1, 0°				M, E1, −20°			
		X	Y	Z	SEQV	X	Y	Z	SEQV	X	Y	Z	SEQV
1.	Molar cusp (NC)	−4.72E-04 (L)	−8.87E-04 (F)	+1.81E-04 (U)	+2.64E-02	−4.24E-04 (L)	−8.75E-04 (F)	+1.19E-04 (U)	+2.68E-02	−3.74E-04 (L)	−8.27E-04 (F)	+4.62E-05 (U)	+2.87E-02
2.	Molar root (NC)	+4.86E-04 (M)	−7.90E-04 (F)	+1.95E-04 (U)	+9.75E-02	+4.67E-04 (M)	−5.92E-04 (F)	+7.63E-05 (U)	+7.05E-02	+5.32E-04 (M)	−6.90E-04 (F)	−3.89E-06 (D)	+4.90E-02
3.	PM cusp (NC)	−4.62E-04 (L)	−9.62E-04 (F)	+4.76E-04 (U)	+9.60E-03	−4.00E-04 (L)	−9.52E-04 (F)	+4.13E-04 (U)	+8.87E-03	−3.35E-04 (L)	−9.04E-04 (F)	+3.26E-04 (U)	+8.04E-03
4.	PM root (NC)	−2.02E-04 (L)	−5.04E-04 (F)	+4.23E-04 (U)	+5.58E-02	−1.76E-04 (L)	−4.92E-04 (F)	+3.66E-04 (U)	+4.81E-02	−1.56E-04 (L)	−4.65E-04 (F)	+2.87E-04 (U)	+3.57E-02
5.	Canine (NC)	−4.19E-04 (L)	−9.37E-04 (F)	+5.59E-04 (U)	+6.93E-03	−3.59E-04 (L)	−9.27E-04 (F)	+4.94E-04 (U)	+6.47E-03	−2.98E-04 (L)	−8.81E-04 (F)	+4.02E-04 (U)	+5.84E-03
6.	CI crown (NC)	−3.54E-04 (L)	−8.25E-04 (F)	+5.03E-04 (U)	+1.43E-03	−2.89E-04 (L)	−8.05E-04 (F)	+4.73E-04 (U)	+1.36E-03	−2.28E-04 (L)	−7.54E-04 (F)	+4.16E-04 (U)	+1.16E-03
7.	CI root (NC)	+7.18E-04 (M)	−1.29E-03 (F)	+6.99E-04 (U)	+5.48E-03	+7.17E-04 (M)	−9.86E-04 (F)	+3.92E-04 (U)	+3.86E-03	+7.90E-04 (M)	−1.14E-03 (F)	+3.74E-04 (U)	+3.31E-03
8.	Zygoma (NC)	+1.70E-04 (M)	−2.51E-04 (F)	−3.99E-04 (D)	+8.97E-02	+1.63E-04 (M)	−1.95E-04 (F)	−3.86E-04 (D)	+6.93E-02	+1.89E-04(M)	−2.19E-04 (F)	−4.77E-04 (D)	+8.07E-02
9.	Orbit (NC)	−3.52E-05 (L)	+1.79E-05 (B)	+4.15E-05 (U)	+7.63E-02	−2.65E-05 (L)	+1.39E-05 (B)	+3.22E-05 (U)	+6.08E-02	−1.56E-05 (L)	+1.09E-05(B)	+2.15E-05 (U)	+4.50E-02
10.	Nasal bone	+3.31E-06 (C)	−3.84E-05 (F)	+8.71E-05 (U)	+2.68E-02	−4.21E-07 (M)	−2.63E-05 (F)	+6.26E-05 (U)	+1.85E-02	+1.79E-06 (C)	−1.89E-05 (F)	+4.77E-05 (U)	+1.53E-02
11.	Subnasale	−2.63E-04 (NC)	−3.34E-04 (F)	−2.25E-04 (D)	+1.73E-02	−2.53E-04 (C)	−3.70E-04 (F)	−2.52E-04 (D)	+1.81E-02	−2.46E-04 (NC)	−3.52E-04 (F)	−2.89E-04 (D)	+1.60E-02
12.	Point A	−1.21E-04 (NC)	−3.34E-04 (F)	+3.85E-04 (U)	+5.64E-03	−9.78E-05 (NC)	−3.17E-04 (F)	+3.58E-04 (U)	+2.92E-03	−8.41E-05 (NC)	−2.93E-04 (F)	+3.11E-04 (U)	+2.17E-03
13.	ANS	−2.26E-05 (NC)	−1.48E-04 (F)	+4.33E-04 (U)	+3.15E-04	−1.35E-05 (NC)	−1.36E-04 (F)	+4.03E-04 (U)	+4.19E-04	−1.68E-05 (NC)	−1.25E-04 (F)	+3.52E-04 (U)	+5.21E-04
14.	PNS	−1.22E-04 (NC)	−2.40E-04 (F)	+4.74E-05 (U)	+3.50E-02	−1.00E-04 (NC)	−2.23E-04 (F)	+3.22E-05 (U)	+3.30E-02	−8.31E-05 (NC)	−2.02E-04 (F)	+1.83E-05 (U)	+3.02E-02
15.	Orbit (C)	+1.44E-04 (L)	+7.20E-05 (B)	+9.30E-05 (U)	+6.48E-02	+1.07E-04 (L)	+5.26E-05 (B)	+7.31E-05 (U)	+5.19E-02	+9.97E-05 (L)	+3.98E-05 (B)	+6.71E-05 (U)	+4.92E-02
16.	Zygoma (C)	+4.49E-04 (L)	−3.23E-04 (F)	+2.41E-04 (U)	+7.81E-02	+3.20E-04 (L)	−2.02E-04 (F)	+1.18E-04 (U)	+2.03E-02	+3.26E-04 (L)	−2.08E-04 (F)	+7.89E-05 (U)	+7.01E-03
17.	CI root (C)	+5.59E-04 (L)	−7.89E-04 (F)	+5.96E-04 (U)	+0.10053	+4.97E-04 (L)	−5.75E-04 (F)	−3.67E-04 (U)	+6.17E-02	+5.44E-04 (L)	−6.53E-04 (F)	+3.39E-04 (U)	+5.67E-02
18.	CI crown (C)	−2.81E-04 (M)	−4.17E-04 (F)	−3.17E-04 (D)	+9.26E-02	−2.75E-04 (M)	−4.09E-04 (F)	−3.48E-04 (D)	+9.84E-02	−2.77E-04 (M)	−3.93E-04 (F)	−3.79E-04 (D)	+8.74E-02
19.	Canine (C)	+7.14E-04 (L)	−1.28E-03 (F)	−8.63E-04 (U)	+4.94E-02	+7.12E-04 (L)	−9.80E-04 (F)	+5.58E-04 (U)	+4.02E-03	+7.83E-04 (L)	−1.14E-03 (F)	+5.68E-04 (U)	+4.74E-03
20.	PM root (C)	+5.56E-04 (L)	−7.77E-04 (F)	+4.79E-04 (U)	+0.12355	+4.94E-04 (L)	−5.67E-04 (F)	+2.82E-04 (U)	+7.45E-02	+5.45E-04 (L)	−6.48E-04 (F)	+2.37E-04 (U)	+6.32E-02
21.	PM cusp (C)	+8.19E-04 (L)	−1.50E-03 (F)	+7.21E-04 (U)	+3.17E-03	+8.31E-04 (L)	−1.16E-03 (F)	+4.47E-04 (U)	+2.42E-03	+9.18E-04 (L)	−1.36E-03 (F)	+4.29E-04 (U)	+2.76E-03
22.	Molar root (C)	+4.99E-04 (L)	−7.36E-04 (F)	+2.53E-04 (U)	+3.55E-02	+4.54E-04 (L)	−5.44E-04 (F)	+1.14E-04 (U)	+2.32E-02	+5.08E-04 (L)	−6.29E-04 (F)	+3.67E-05 (U)	+1.83E-02
23.	Molar cusp (C)	+8.40E-04 (L)	−1.56E-03 (F)	+2.55E-04 (U)	+2.77E-02	+8.55E-04 (L)	−1.21E-03 (F)	+4.38E-05 (U)	+2.18E-02	+9.56E-04 (L)	−1.42E-03 (F)	−6.12E-05 (U)	+3.09E-02

Analysis was carried out using ANSYS 19; Inc., Canonsburg, PA. Displacement was measured in mm. Stress was measured in N/mm.^{2} M (600 g/side) represented MG force, E1 (=250 g) represented SME force. Along X-axis, cleft side: negative value indicated medial movement (M) and positive value indicated lateral movement (L), noncleft side: Positive value indicated medial movement (M) and negative value indicated lateral movement (L). Midline structures: negative value indicated noncleft movement (NC) and positive value indicated cleft side movement (C). Along Y-axis: negative value indicated forward movement (F) and positive value indicated backward movement (B). Along Z-axis: negative value indicated downward movement (D) and positive value indicated upward movement (U), von Mises stress (=SEQV): negative sign indicated compressive stress, positive sign indicated tensile stress. Abbreviations used: MG: Maxgym, SME: slow maxillary expansion, C: cleft, NC: noncleft, ANS: anterior nasal spine, PM: premolar, CI: center incisor.
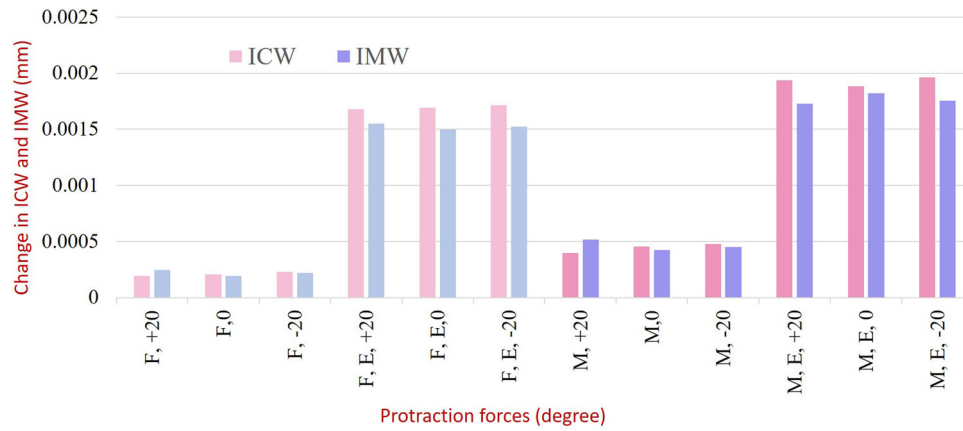
Figure 11. Graph showing change in ICW and IMW for FM and MG therapy with and without expansion. Abbreviations used: ICW: intercanine width, IMW: intermolar width, FM (*F*): facemask, MG (*M*): Maxgym.
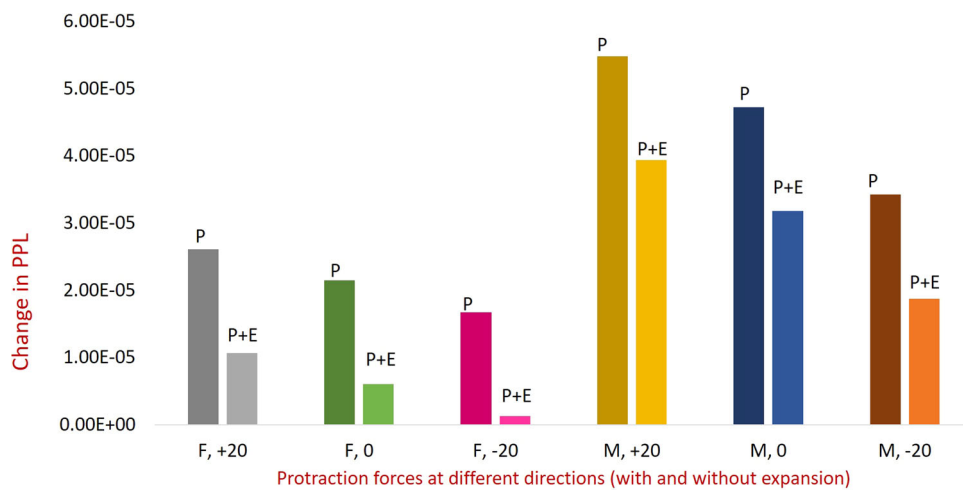

Figure 12. Graph showing change in PPL for protraction forces using FM and MG at +20?, 0?, and −20? Palatal plane is the distance between the ANS and PNS. Abbreviations used: *P*: protraction, *F*: facemask, *M*: Maxgym, *E*: expansion, PPL: palatal plane length, ANS: anterior nasal spine, and PNS: posterior nasal spine.
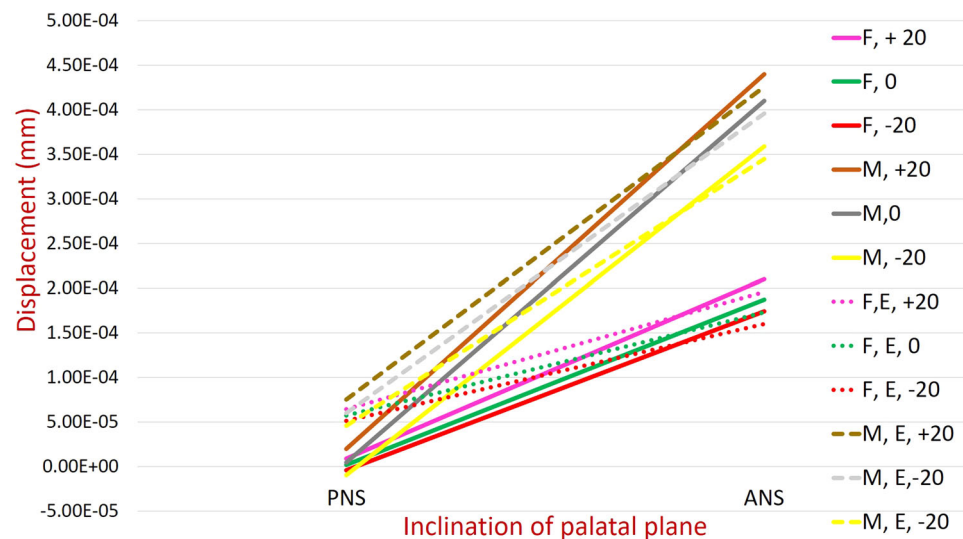

Figure 13. Graph showing inclination of PP for FM and MG forces at +20°, 0?°, and −20?° Palatal plane is the distance between the ANS and the PNS. Abbreviations used: FM (*F*): facemask, MG (*M*): Maxgym, E2 (*E*): rapid maxillary expansion, PP: palatal plane, ANS: anterior nasal spine, and PNS: posterior nasal spine.

Disclosure statement

There is no potential conflict of interest to disclose.

ORCID

Shahistha Parveen http://orcid.org/0000-0002-5984-6719

References

Buschang PH, Porter C, Genecov E, Genecov D, Sayler KE. 1994. Face mask therapy of preadolescents with unilateral cleft lip and palate. Angle Orthod. 64(2):145–150.

Chen Z, Pan X, Shao Q, Chen Z. 2013. Biomechanical effects on maxillary protraction of the craniofacial skeleton with cleft lip and palate after alveolar bone graft. J Craniofac Surg. 24(2):446–453.

Chen Z, Pan X, Zhao N, Chen Z, Shen G. 2015. Asymmetric maxillary protraction for unilateral cleft lip and palate patients using finite element analysis. J Craniofac Surg. 26(2):388–392.

Cobourne MT. 2004. The complex genetics of cleft lip and palate. Eur J Orthod. 26(1):7–16.

Dogan S. 2012. The effects of face mask therapy in cleft lip and palate patients. Ann Maxillofac Surg. 2(2):116.

Eom J, Bayome M, Park JH, Lim HJ, Kook Y-A, Han SH. 2018. Displacement and stress distribution of the maxillofacial complex during maxillary protraction using palatal plates: A three-dimensional finite element analysis. Korean J Orthod. 48(5):304–315.

Gautam P, Valiathan A, Adhikari R. 2009. Maxillary protraction with and without maxillary expansion: A finite element analysis of sutural stresses. Am J Orthod Dentofacial Orthop. 136(3):361–366.

Grandori F, Merlini C, Amelotti C, Piasente M, Tadini G, Ravazzani P. 1992. A mathematical model for the computation of the forces exerted by the facial orthopedic mask. Am J Orthod Dentofacial Orthop. 101(5):441–448.

Hata S, Itoh T, Nakagawa M, Kamogashira K, Ichikawa K, Matsumoto M, Chaconas SJ. 1987. Biomechanical effects of maxillary protraction on the craniofacial complex. Am J Orthod Dentofacial Orthop. 91(4):305–311.

Holberg C, Holberg N, Schwenzer K, Wichelhaus A, Rudzki-Janson I. 2007. Biomechanical analysis of maxillary expansion in CLP patients. Angle Orthod. 77(2): 280–287.2.0.CO;2] [17319763]

Itoh T, Chaconas SJ, Caputo AA, Matyas J. 1985. Photoelastic effects of maxillary protraction on the craniofacial complex. Am J Orthod. 88(2):117–124.

Kawakami M, Yagi T, Takada K. 2002. Maxillary expansion and protraction in correction of midface retrusion in a complete unilateral cleft lip and palate patient. Angle Orthod. 72(4):355–361.

Keles A, Tokmak EC, Erverdi N, Nanda R. 2002. Effect of varying the force direction on maxillary orthopedic protraction. Angle Orthod. 72(5):387–396.

Liao Y-F, Mars M. 2005. Long-term effects of palate repair on craniofacial morphology in patients with unilateral cleft lip and palate. Cleft Palate Craniofac J. 42(6): 594–600.

Mathew A, Nagachandran KS, Vijayalakshmi D. 2016. Stress and displacement pattern evaluation using two different palatal expanders in unilateral cleft lip and palate: A three-dimensional finite element analysis. Prog Orthod. 17(1):38.

Molsted K, Dahl E. 1987. Face mask therapy in children with cleft lip and palate. Eur J Orthod. 9(3):211–215.

Moon W, Wu KW, MacGinnis M, Sung J, Chu H, Youssef G, Machado A. 2015. The efficacy of maxillary protraction protocols with the micro-implant-assisted rapid palatal expander (MARPE) and the novel N2 mini-implant: A finite element study. Prog Orthod. 16(1):16.

Proffit WR, Fields HW, Sarver DM, Ackerman JL. 2013. Contemporary orthodontics. 5th ed. St. Louis (MO): Elsevier/Mosby.

Tanne K, Hiraga J, Sakuda M. 1989. Effects of directions of maxillary protraction forces on biomechanical changes in craniofacial complex. Eur J Orthod. 11(4):382–391.

Tanne K, Sakuda M. 1991. Biomechanical and clinical changes of the craniofacial complex from orthopedic maxillary protraction. Angle Orthod. 61(2):145–152.

Tindlund RS. 1994. Skeletal response to maxillary protraction in patients with cleft lip and palate before age 10 years. Cleft Palate Craniofac J. 31(4):295–308.

Tortop T, Keykubat A, Yuksel S. 2007. Facemask therapy with and without expansion. Am J Orthod Dentofacial Orthop. 132(4):467–474.

Turley PK. 1988. Orthopedic correction of Class III malocclusion with palatal expansion and custom protraction headgear. J Clin Orthod. 22(5):314–325.

Vaughn GA, Mason B, Moon H-B, Turley PK. 2005. The effects of maxillary protraction therapy with or without rapid palatal expansion: A prospective, randomized clinical trial. Am J Orthod Dentofacial Orthop. 128(3): 299–309.

Yan X, He W, Lin T, Liu J, Bai X, Yan G, Lu L. 2013. Three-dimensional finite element analysis of the craniomaxillary complex during maxillary protraction with bone anchorage vs conventional dental anchorage. Am J Orthod Dentofacial Orthop. 143(2):197–205.

Yang I-H, Chang Y-I, Kim T-W, Ahn S-J, Lim W-H, Lee N-K, Baek S-H. 2012. Effects of cleft type, facemask anchorage method, and alveolar bone graft on maxillary protraction: A three-dimensional finite element analysis. Cleft Palate Craniofac J. 49(2):221–229.

Yepes E, Quintero P, Rueda ZV, Pedroza A. 2014. Optimal force for maxillary protraction facemask therapy in the early treatment of class III malocclusion. Eur J Orthod. 36(5):586–594.

Yu HS, Baik HS, Sung SJ, Kim KD, Cho YS. 2007. Three-dimensional finite-element analysis of maxillary protraction with and without rapid palatal expansion. Eur J Orthod. 29(2):118–125.

Zhang D, Zheng L, Wang Q, Lu L, Ma J. 2015. Displacements prediction from 3D finite element model of maxillary protraction with and without rapid maxillary expansion in a patient with unilateral cleft palate and alveolus. Biomed Eng Online. 14:80.